63-3-4

403 667

PROGRESS REPORT
FOR
DEC., 1962, JAN., FEB., 1963

Coordinated Science Laboratory

UNIVERSITY OF ILLINOIS - URBANA, ILLINOIS

PROGRESS REPORT
FOR
DEC., 1962, JAN., FEB., 1963

COORDINATED SCIENCE LABORATORY
UNIVERSITY OF ILLINOIS
URBANA, ILLINOIS

Contract DA-36-039-TR US AMC 02208(E)
DA Project 3A-99-25-004

The research reported in this document was made possible by support extended to the University of Illinois, Coordinated Science Laboratory, jointly by the Department of the Army, Department of the Navy (Office of Naval Research), and the Department of the Air Force (Office of Scientific Research) under Department of Army Contract DA-36-039-TR US AMC 02208(E).

APRIL 24, 1963

COORDINATED SCIENCE LABORATORY

ABSTRACT OF

PROGRESS REPORT FOR DECEMBER 1962, JANUARY, FEBRUARY, 1963

1. Electric Vacuum Gyroscope

The analysis of slow-down and precession torques resulting from radial mass unbalance of an electric vacuum gyroscope rotor is described. Continued experiments on the verification of torques resulting from deformed rotor translational misalignment are described and the results given.

2. Surface and Atomic Physics

The pressure shift of the hyperfine structure of atomic nitrogen N^{14} in the ground state has been investigated for the following buffer gases: molecular nitrogen, helium, neon and argon.

3. Computers

Operation statistics, logic modifications, and programming efforts are reported for the CSX-1. For the CDC 1604, operation statistics are given. Studies in which a computer plays both roles in a game are reported. Provisions by which a computer may produce multivoiced music is reported. An abstract of a recent report on Automatic Air Traffic Control is presented.

4. System Theory

Various results related to control optimization and feedback theory were obtained. Various computer programs necessary for contact network synthesis, self-diagnosis, and graph theory were completed. Further results on self-repair and on communication nets were also obtained.

5. PLATO

In January 1963, ILLIAC was removed from service. The computer control for PLATO was switched from the ILLIAC to the CDC 1604 located at the Coordinated Science Laboratory. Two teaching logics using PLATO Laboratory were completed. One is used for demonstration purposes to illustrate the teaching of Archimedes Principle by simulated laboratory experiments. The other logic will be used for inquiry training. Preliminary analysis of student electrocardiogram data indicates that student-discovery is reflected in the heart rate. Testing of the PLATO III equipment was started this quarter.

6. Vacuum Instrumentation

Study of sticking probability of N_2 using partial pressure gauges has continued. A study of the anomalous behavior of the Bayard-Alpert gauge at very low pressure was begun this quarter, using both partial and total pressure gauges.

7. Plasma Physics

Although Nordsieck's method of solution of the Boltzmann equation for a shock wave appears, by most criteria, to be successful, the Monte Carlo calculation of the collision integral is biased. A series of new routines has therefore been developed that will permit efficient study of the collision integral calculations. The momentum transfer cross section for electrons colliding with Neon atoms was measured as a function of temperature in the range 200 - 600° K. The results indicate a minimum in the cross section at 0.11 eV. An experiment has been performed to demonstrate the incoherent scattering of microwaves from a plasma. A resonance was found when the frequency of the scattered radiation corresponded to the sum of incident frequency plus plasma frequency. A new improved model of the plasma delay line has been constructed that should result in a better focusing of the electrons and provide more experimental flexibility.

8. High Magnetic Field Superconductors

Measurements have been made of the critical current as a function of temperature and magnetic field of single crystalline vanadium and compared with measurements on similar material which has been cold worked. Clusters of Nb_3Sn crystals have been grown from saturated solutions of Nb in Sn at temperatures between 1,000°C and 1,250°C. Some developments in fabrication of Nb_3Sn wire have been made in cooperation with the Fansteel Metallurgical Corporation.

9. Vacuum Electrical Breakdown

The preliminary measurements previously reported have been repeated with greater care. The electron microscope studies have been continued.

10. Physical Electronics

The voltage-current characteristics of metal-oxide-metal sandwiches have been studied.

11. Arms Control and Disarmament Research

Beginning part-time studies, in cooperation with faculty from other departments, are reported.

PUBLICATIONS AND REPORTS

1. Journal Articles Published or Accepted

- S. J. Kahne, "Note on Two Point Boundary Value Problems," IEEE Transactions on Automatic Control, to be published, July, 1963.

2. Meeting Papers Presented

P. G. Braunfeld, Computer Programs for Automatic Teaching Devices. Digital Computer Laboratory Colloquium, University of Illinois, March, 1963.

S. J. Kahne, "A Constraint Mapping Technique for System Optimization," IEEE Convention Record, 1963 (to appear).

S. J. Kahne, "Note on Two Point Boundary Value Problems," CSL Report I-120, February, 1963.

M. Sobral, Jr., "Stability Considerations in the Synthesis of Time-Varying Feedback Systems," presented at the IEEE Winter General Meeting, January 29, 1963, New York.

3. Technical Reports

R-157 On Physical Realizability of Signal Flow Graphs and Realization Techniques, Manohar Lal, December, 1962.

R-158 Realizability Conditions of Single-Contact Networks, Shu-Park Chan, December, 1962.

R-160 The Use of an Automatic Computer System in Teaching, P. G. Braunfeld and L. D. Fosdick.

4. Book Reviews

S. J. Kahne, "Stability by Lyapunov's Direct Method," by Lefschetz and LaSalle, Pi Mu Epsilon Journal, vol. 3, no. 7, pp. 348-349.

COORDINATED SCIENCE LABORATORY

Personnel

Faculty and Research Associates

Allen, D. R.
Alpert, D., Director
Anderson, R. W.
Bitzer, Donald L.
Bohmer, H.
Braunfeld, P. G.
Brown, R. M.
Chan, S. P.
Chen, C. L.
Cooper, D. H.
Cruz, J. B.
Desmond, J. J., Ass't. Director
Diamond, D.
Divilbiss, J. L.
Elliott, B.
Elsey, J. C.
Frauenfelder, H., Assoc. Director
Gooch, J. D.
Gourishankar, V.
Hicks, B. L.
Hoffman, J.
Kahne, S.
Kansky, R. J.
Kirkwood, B. D.
Knoebel, H.
Kopplin, J. O.
Krone, H. V.
Kruus, J.
Kypta, L. S.
Lee, D. A.
Lichtenberger, W. W.
Luscher, E.
Lyman, Ernest
Lyman, Elisabeth
Mayeda, W.
Narayanasamy, R.
Peacock, R.
Perkins, W.
Propst, F.
Prothe, W.
Raether, M.
Resh, J.
Ruina, J. P. (on leave)
Skaperdas, D. O.
Satterthwaite, C. B.
Segovia, J.
Seshu, Sundaram
Slottow, H. G.
Srivastava, S. P.
Stein, H.
Stifle, J. E.
Tomaschke, H. E
Trogdon, R. L.
Van Valkenburg, M. E., (on leave) Assoc. Director
Voth, Brian
Wax, Nelson

Research Assistants

Aggarwal, J. K.
Barger, A. R.
Bennett, S. A.
Blomme, R.
Brown, O. Robert
Carr, Wayne
Chang, Herbert Y.
Chen, W. K.
Cooper, T.
Crowder, James
Cummings, James
Franz, Frank
Govaia, James
Harris, John
Jenks, Richard
Leung, W. C.
Levine, M.
Levitt, M.
Lie, T.
Mendel, C.
Morgan, Lezlie
Murata, T.
Piper, Thomas
Ponzo, P. J.
Resh, James
Schuemann, W. C.
Secrest, M.
Smith, D. W.
Sobral, M.
Snyder, D. P.
Srivastava, S. P.
Tibbetts, G.
Tsui, J. B.
Willson, R. H.
Wise, F.
Wisman, E. C.

Accountant

Klein, N.

Secretary

Gschwendtner, J.

Typists and Stenos

Berger, J.
Groo, B.
Harris, M.
McDonald, R.
Schulze, B.
Seavey, K.

Instrument Makers

Merritt, K. E.
Zackery, R. L.

Res. Engineering Asst.

Powers, N. T.

Procurement and Supply

Rumbaugh, E. E.

Storekeepers

Drews, C. E.
Lofton, C.

Electronic Technicians

Bowers, J.
Casale, T.
Coad, D. E.
Cooper, G.
Crawford, G.
Deschene, D. R.
Hedges, L.
Holy, F. O.
Jordan, H.
Knoke, J. G.
Lawrence, W. I.
Popeney, T. W.
Roberts, G.
Schmidt, W.
Simpson, L.
Streff, L. W.
Turpin, H. G.

Accounting Clerk

Potter, R. E.

Photographer

Fillman, W.

Draftsmen

MacFarlane, R. F.
Tewes, A. F.

Laboratory Mechanics

Beaulin, W. E.
Bouck, G.
Burr, J. G.

Electronics Engr. Asst.

Carter, E. N.
Gardner, O. E.
Neff, E. H.
Vassos, N.

Glassblower

Lawrence, W.

Student Assistants

Altenbernd, N.
Artman, J. B.
Benden, L.
Cattoir, R.
Curren, R.
Doyle, J.
Evans, K.
Ewen, D.
Fierstein, G.
Goldstein, J.
Kent, D.
Klingbeil, R.
Konrad, F.
McGinness, L.
Metze, V.
Mitchell, J.
Nagel, D.
Pratt, J.
Quillman, W.
Riddle, G.
Ries, R.
Robinett, D.
Sandorfi, G.
Singer, S.
Thomas W. B.
Troue, H. H.
Usiewicz, J.
Utsumi, T.
Warnes, R.
Wright, F.

Physical Sciences Staff Asst

Thrasher, W.

TABLE OF CONTENTS

CONTENTS (Continued)

1. ELECTRIC VACUUM GYROSCOPE

H. W. Knoebel
D. O. Skaperdas
D. Allen
R. W. Anderson
J. D. Gooch
B. D. Kirkwood
V. Krone
D. Lee
W. C. Prothe

1.1 Introduction

The electric vacuum gyroscope, a high-precision inertial navigation instrument employing a coasting spherical metal rotor supported without physical contact in vacuum by electric fields, is being investigated. The objectives are (1) to obtain a complete understanding of subtle effects which may influence the design of ultra-high precision electric vacuum gyroscopes and (2) to develop new techniques for gyro improvement.

Long term experiments using two different gyro test setups are being conducted to experimentally verify predicted small changes in performance resulting from various parameter adjustments.

1.2 Gyro Torque Analysis

A complete analysis of the sources of precession and slow-down torques on the electrically supported gyro should include the effects of rotor mass unbalance[1]. The mass center and geometric center do not coincide in general, and a vector specifying the location of the geometric center with respect to the mass center has two components, one parallel to the spin axis and the other normal to it. Consideration of the two is best done separately.

The parallel component produces the classical mass-unbalance precession torque which appears because acceleration forces on the rotor converge at the mass center while the electric forces converge at the geometric center, and a torque couple is created. The analysis of the effect of this torque on gyro performance is straightforward and is not discussed here, but the effect of the radial component is more subtle.

Precession torques may occur indirectly because of radial unbalance. The rotor tends to spin about an axis which passes through the mass center, but the support servos tend to force the rotor to spin about an axis through its geometric

---

[1] Minneapolis-Honeywell Reports: 1515-QR1 (July, 1959), 1901-QR4 (March, 1960), 1901-TR1 (April, 1961).

center. In general, the spin axis passes through some other point which varies with the spin speed: at very low speeds the servos win control, and the rotor spin axis passes through the geometric, and, at very high speeds, the servos lose control and the spin axis passes through the mass center.

First, assume an infinite number of electrodes and let each diametrically opposing pair have its own push-pull support servo. As the spherical rotor spins about some axis not through the geometric center, each electrode pair "sees" a sinusoidally varying gap. Most servos sense the gap through the accompanying capacitance of the electrode to the rotor. The sensed signal is amplified, frequency compensated to provide stability, and then converted to a correction voltage which is applied to the electrode which, in turn, applies a corrective force on the rotor. The servo feedback frequency response is specified by a gain or stiffness (force per unit gap change) and a phase angle between output force and gap change.

If the frequency response of all servos is identical, then an analysis shows that there are no precession torques, but there is the slow-down torque. The integrated value of this torque is

$$T = -\frac{4\pi}{3} K\rho^2 a \sin\zeta,$$

where T is the torque (dyne cm),

K is the servo gain (force per unit area/fractional gap change),

ρ is the radial distance between actual spin axis and a line through the geometric center (cm),

a is the sphere radius (cm), and

ζ is the servo phase angle.

At rotor speeds where the servo output response leads the gap change ($\zeta > 0$) the rotor slows, but when $\zeta < 0$, the rotor accelerates. It follows that if all support servos are not identical, precession torques appear.

Consider the more practical case of electrodes placed symmetrically over the sphere, either in the pattern of the regular polyhedron or, if a large number of electrodes is desired, in the pattern obtained when the spherical faces of the regular polyhedrons are broken up into sub-faces. Consider the torque from one electrode, which may be written as two torques--a slow-down and a precession torque:

$$T_{slow\ down} = -\frac{\Omega}{6} K\rho^2 a \sin^2\Psi \sin\zeta,$$

$$\underset{\sim}{T}_{precession} = -\frac{\Omega}{12} K\rho^2 a \sin 2\Psi(\underset{\sim}{i} \sin\zeta + \underset{\sim}{j} \cos\zeta),$$

where Ω is a function of the solid angle subtended by the electrode,

Ψ is the angle of the spin axis from a radial line to the center of the electrode,

$\underset{\sim}{i}$ is a unit vector in the plane in which Ψ is measured and normal to the spin axis,

and $\underset{\sim}{j}$ is a unit vector normal to the plane in which Ψ is measured.

Both torques are functions of the angular location of the spin axis with respect to the electrode, and both functions are symmetric; i.e., the torques from one electrode and the electrode diametrically opposite add. After adding the contribution of the slow-down torque from all electrode pairs, the total torque is less than, but approaches, the torque calculated in the infinitely many electrode case.

The individual electrode precession torques are of the same form as the second-order rotor distortion torques, except that, in this case, their magnitudes and directions depend on the servo gain and phase parameters, which are a function of spin speed. The total torque will vanish if the frequency characteristics of all support servos are identical.

A complete analysis of this work is being included in a comprehensive report on electric vacuum gyroscope precession torques by D. Allen to be published during the next quarter.

D. Allen

1.3 Gyro Rotors

It was reported in the last quarter that degassing from two rotors manufactured by the American Beryllium Company prevented their use in a gyro system. Mild bakeouts did not clean up the rotors, nor did sonic cleaning of one of them decrease its degassing rate.

Two other beryllium rotors, also fabricated by American Beryllium, were sent to Speedring Corporation of Warren, Michigan, for balancing. After a brief attempt at balancing, these two rotors were returned to us with a notation that many small surface pit holes were being uncovered during lapping and that these pits loaded with lapping compound and caused a tearing condition. The previously mentioned rotor degassing may be due to minute pit holes which have trapped lapping compounds or other machine shop residues. Regardless of its nature, this is not a basic problem since excellent rotors are obtained from Minneapolis-Honeywell.

1.4 Gyro Test Data

Previous runs concentrated on measuring the effects of a constant displacement of a centrifugally deformed rotor with respect to its electrodes in the $\underset{\sim}{i}$ and $-\underset{\sim}{i}$ direction[2]. It was shown that the experimental results corroborated the theoretical predictions; namely, that for this type of rotor displacement the spin axis locus should show spiraling and culmination shifts, with the closure time not affected. The theoretical results were shown in graphical form in Fig. 1 of the previous progress report. As a summary for the series of runs 56B, C, and D, the predicted ratio of the culmination shift to the spiraling rate per day for a 15^{o} coning radius about north, as obtained from Fig. 1 of the previous progress report, is $420/350 = 1.2$. The ratio actually measured was 1.3 ± 0.1, the error being attributed to the difficulty in accurately determining the culmination point. The spiraling and culmination shift directions also agreed with theory.

In the past quarter, an excellent beryllium rotor, fabricated and balanced by Minneapolis-Honeywell, was tested. In the series of runs 63 A, B, and C the centrifugally distorted rotor was given a constant displacement with respect to its electrodes in the $\underset{\sim}{j}$ and $-\underset{\sim}{j}$ directions (see Fig. 1, Progress Report for Dec., 1961, Jan. and Feb., 1962). The theoretical results for this type of displacement, obtained by solving equations 1.1 and 1.2 of the previous progress report on a digital computer, are plotted in Fig. 1.1. It is to be noted here that the closure time and elongation shifts are affected and that no spiraling takes place. The curves show the predicted elongation shift and closure time difference, from one sidereal day, versus the nominal angle at which the spin axis cones about north. The curve for elongation shift is antisymmetric, and that for the closure time difference is symmetric about the 90^{o} point. In runs 63 A, B, and C, the nominal coning radius was 22.5^{o}. From Fig. 1.1, the predicted ratio of the closure time difference to the elongation shift for a coning radius of 22.5 degrees is $5320/305 = 17.4$. The actual ratio measured was 17.2 ± 1.2, the error again being attributed to the difficulty

[2] Fig. 1, Progress Report for Dec. 1961, Jan. and Feb., 1962.

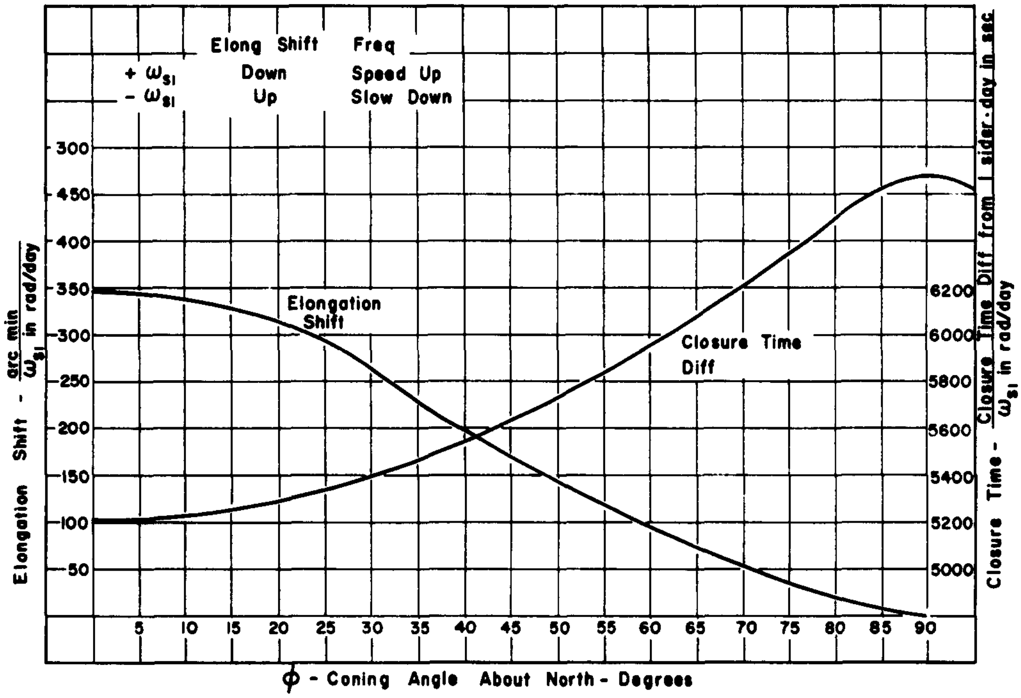

Figure 1.1. Theoretical Effects of Translation.

in accurately determining the elongation point. The directions of the elongation shifts and the closure time differences agreed with those indicated in Fig. 1.1.

Since we have previously qualitatively corroborated the effect of a constant rotor displacement in the $\underset{\sim}{k}$ direction, showing that it is equivalent to a change in mass unbalance, we should now be able to predict the effects of any constant displacement of a centrifugally deformed (first and second order distortion) rotor with respect to its electrodes.

The knowledge gained during the previous quarter was used in an attempt to "tune up" the beryllium gyro rotor described above. In other words, a series of experiments were performed using a theoretically determined adjustment to correct for mass unbalance, sag and non-centering of the rotor. The rotor was successively given constant displacements with respect to its electrodes in the $\underset{\sim}{i}$, $\underset{\sim}{j}$, and $\underset{\sim}{k}$ directions with expected changes in spiraling rates and closure time differences. The rotor rotation frequency was kept at a low 110 rps in order to minimize damage in case of a levitation failure. Consequently, the drift rate due to mass unbalance was too large to cancel out by displacing the rotor a nominal amount along its spin axis ($\underset{\sim}{k}$ direction). Changes in closure time of 2-1/2 minutes were easily obtained and the spiraling could be changed in either direction or eliminated. A failure in the levitation system terminated this experiment. The effects of this accident on the rotor are now being investigated.

D. Skaperdas

2. SURFACE AND ATOMIC PHYSICS

Surface	Atomic
E. Lüscher	E. Lüscher
H. Böhmer	F. Franz
H. Frauenfelder	N. Levine
F. Propst	D. Smith
T. Cooper	T. Piper
G. Tibbetts	

2.1 Pressure Shift of the Atomic Nitrogen Hyperfine Structure

The pressure shift of the hyperfine structure of atomic nitrogen 14 in the $(2p)^3\ {}^4S_{3/2}$ electronic ground state with molecular nitrogen, helium, neon, and argon as buffer gases has been investigated. Buffer gas pressures ranged from 7 Torr to 87 Torr. The results complement previous studies made both at Harvard[1,2] and at Illinois.[3,4]

Oriented atomic nitrogen was obtained through spin exchange with optically pumped cesium vapor using the flow technique described by Holloway, et al.,[4] with several improvements. The a.c. magnetic field compensation has been improved according to a suggestion from Lambert,[5] resulting in a narrower resonance line width, hence providing more accurate results. The dissociation of molecular nitrogen was effected by a new gaseous discharge utilizing stainless steel electrodes powered by a 100 watt 1.5 mm/sec oscillator. Finally, a cesium light source[6] with considerably greater D_1 intensity than previously available was constructed, providing a much better signal-to-noise ratio.

From all observed nitrogen hyperfine transitions, the least field dependent ($F = 3/2$, $m_F = \pm 3/2 \rightarrow F = 1/2$, $m_F = \pm 1/2$) were chosen in order to provide the most accurate determination of the frequency shift. Measurement were made at twelve different values of pressure for each buffer gas, with an average of ten readings per data point. The average standard deviation for any one of

---

1 R. H. Lambert and F. M. Pipkin, Bull. Amer. Phys. Soc. 7, 26 (1962).

2 R. H. Lambert and F. M. Pipkin, Phys. Rev. 129, 1233 (1963).

3 W. W. Holloway, Jr., E. Lüscher, and R. Novick, Bull. Amer. Phys. Soc. 7, 26 (1962).

4 W. W. Holloway, Jr., E. Lüscher, and R. Novick, Phys. Rev. 126, 2109 (1962).

5 R. H. Lambert, private communication.

6 R. G. Brewer, Rev. Sci. Instrum. 32, 1356 (1961).

these points is less than 15 cps. The results of these measurements are represented in Table I, while a comparison of the experimental results with the theoretical values calculated by Adrian[7] is presented in Table II. All readings with helium, neon, and argon as buffer gas were made with the same constant amount of 3.0 ± 0.5 Torr of nitrogen in the system. The zero pressure intercepts for helium and neon must therefore be shifted down by 7 cps, and 6 cps, respectively, while the corresponding slopes remain unaffected. The corrected curves are graphed in Fig. 2.1. The average of the values for the zero pressure splitting is 15 676 374 ± 10 cps, compared with the value given by Lambert and Pipkin[2] of 15 676 392 ± 6 cps for helium only, and the value given by Holloway, et al.[4] of 15 676 390 ± cps, for nitrogen only. There is fairly good agreement in this experimental data. The zero pressure splittings had not been measured before in the presence of neon or argon. Unfortunately, we were not able to observe the nitrogen resonances using krypton or xenon as buffer gas.

E. Lüscher
F. A. Franz
D. W. Smith

---

[7] F. J. Adrian, Phys. Rev. 127, 837 (1962).

Table I

Buffer Gas	Pressure Range (mm Hg)	$\nu_o(F = 3/2 \rightarrow F = 1/2)$ (cycles/sec)	$\langle d\nu/dp \rangle$ (c/sec mm Hg)
He	19.9 - 86.1	15,676,380 $\pm$ 8	0.18 $\pm$ 0.056
Ne	14.2 - 87.0	15,676,379 $\pm$ 10	0.365 $\pm$ 0.060
Ar	10.9 - 53.6	15,676,381 $\pm$ 8	2.56 $\pm$ 0.09
N_2	6.7 - 85.0	15,676,369 $\pm$ 10	2.49 $\pm$ 0.05

Values of the zero pressure intercepts and slopes of the frequency vs buffer gas pressure curves for the ($F = 3/2 \rightarrow F = 1/2$) hyperfine transition, as derived from a least squares fit to the experimental data. Several of the zero pressure intercepts must be adjusted, as is explained in the text. Errors quoted are equal to two standard deviations from the mean.

Table II

Effect of Various Buffer Gases on the Nitrogen Hyperfine Splitting Constant

Buffer Gas	$\left\langle \frac{dA_N^{14}}{dp} \right\rangle_{exp}$ (c/sec mm Hg)	$\left\langle \frac{dA_N^{14}}{dp} \right\rangle_{theory}$ (c/sec mm Hg)	$\left(\frac{dA}{dp}\right)_{exp} / \left(\frac{dA}{dp}\right)_{theory}$
He	0.121 $\pm$ 0.037	1.1	0.11
Ne	0.244 $\pm$ 0.040	1.8	0.14
Ar	1.71 $\pm$ 0.06	5.0	0.34
N_2	1.66 $\pm$ 0.03	4.8	0.34

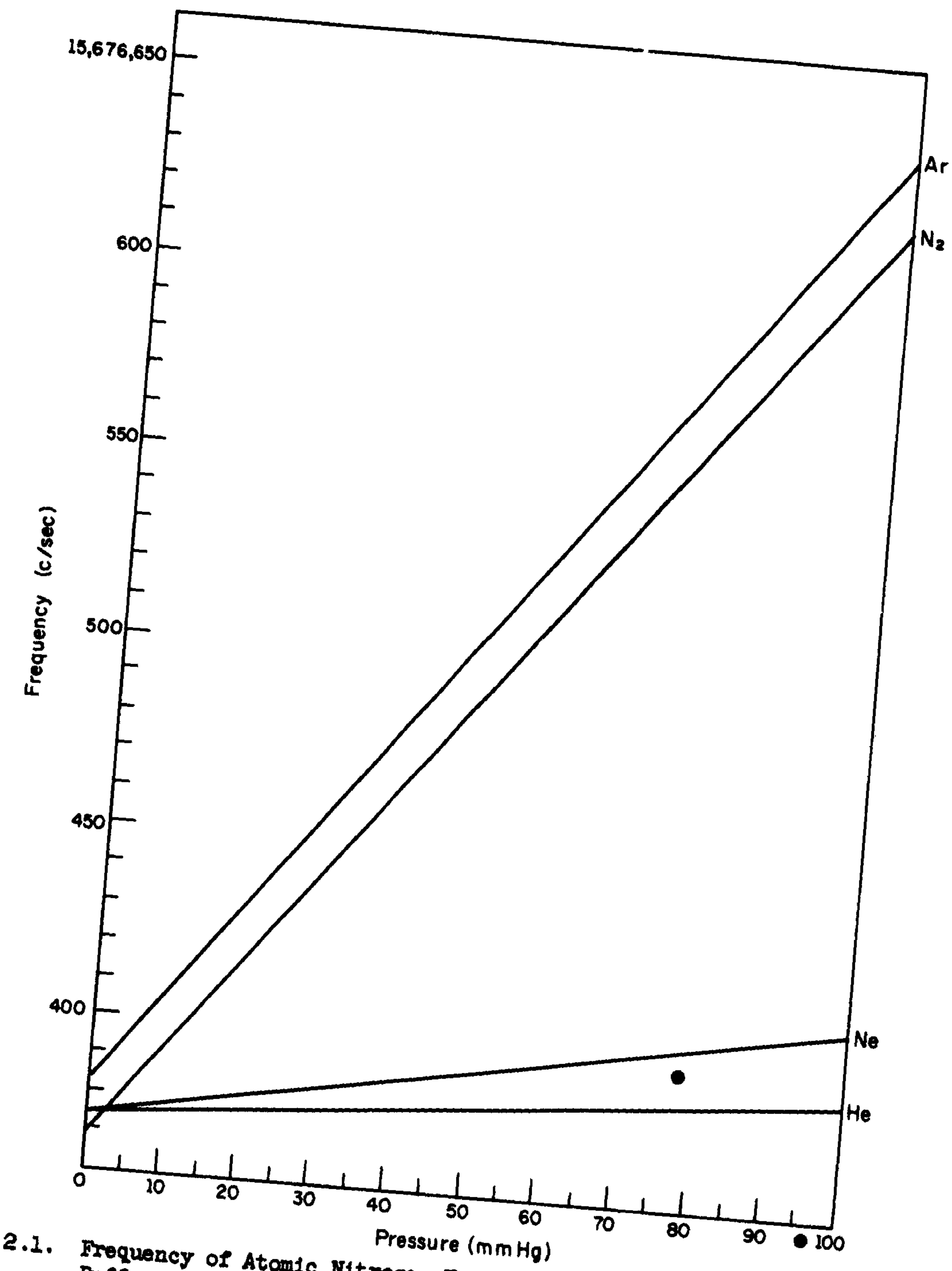

Figure 2.1. Frequency of Atomic Nitrogen Hyperfine Transitions as a Function of Buffer Gas Pressure.

3. COMPUTER

R. M. Brown
D. H. Cooper
J. Divilbiss
J. Govaia
R. Jenks
L. Kypta
M. Levitt
W. W. Lichtenberger
P. Ponzo
S. Srivastava
J. Stifle
R. Trogdon
F. Wise
N. Wax

3.1 Introduction

This division is concerned with the design and application of digital computers for information processing, primarily in the areas of real time and non-numerical operations. The present work lies in three areas: the development and supervision of the CSL computing facilities centering on the CSX-1 and a CDC 1604 computer, and studies in artificial intelligence.

3.2 CSX-1 Computer

3.2.1 Operations

Period: November 29, 1962 to February 28, 1963

Total Running Time	449.5 hrs	
Ave. per day (5 day week)	6.9 hrs	
Scheduled Maintenance Time	0.0 hrs	
Emergency Maintenance Time	1.2 hrs	(.27 o/o)
Operational Time	448.3 hrs	(99.73 o/o)
Breakdown of Emergency Maintenance Time		
Cold Solder Joint	1 hr	
Replace 6 transistors	.2 hr	

The computer was shut down for five weeks during this quarter for the installation of the V = 7 modification (see below) and a temperature sensing unit. The transistor failures mentioned above occurred during the installation and checkout of the temperature sensing unit. They were in three driver stages.

3.2.2 Logic Modifications

The V = 7 modification affects those orders for which the V or n bits refer to an accumulator. For these orders if V or n is identically seven, the word or words immediately following the order in the program specify memory locations. The effect of this modification is to permit any memory located to be designated as an accumulator and processed accordingly.

In addition to V = 7 modifications the following changes in the order code are being made.

Addition of input and output orders directly to and from memory

Addition of bit-compliment orders

Removal of the two logical sum orders and replacing them with two special masked compare orders

Modification of the existing compare orders

Addition of a memory increment order.

Details of these changes along with the V = 7 modification will appear in a new CSX-1 manual.

J. Stifle
R. Trogdon

3.2.3 Programming

A new CSL-1 simulator, SACSIM2, was written for the CDC 1604 in order to accomodate the modifications in the order code. This program enables programs written in the new order code to be assembled and checked-out prior to the completion of hardware modifications.

The CSX-1 assembly program, SAC, is currently being revised to make input format more flexible and compatible with 1604 assembly programs. The major modifications to the assembler, scheduled for completion during the next quarter, permit the following:

1. The use of symbolic addresses consisting of up to eight alphanumeric characters.
2. Mnemonic codes of up to nine alphabetical characters (normally three).
3. New input-output "macro-instructions" similar to those used in Fortran.
4. Format statements associated with these macro-instructions which also may be used for packing binary data into program words.

Routines to read and write magnetic tape, and output to the 1612 printer were completed. The routine "COPY" which takes input from any input channel and reproduces it on any output channel has been completed and checked out.

R. M. Brown
R. D. Jenks
F. G. Wise

3.3 CDC 1604 Computer

3.3.1 Operations

Period: December 1, to February 28, 1963

Total Running Time: 986.5 hours

Average per day (five day week) 15.91 hours

Average per day (including Saturday, Sunday and holidays) 10.96 hours

Operational Time: 913 hours (92.55 o/o)

Preventive Maintenance Time: 69 hours (6.99 o/o)

Emergency Maintenance Time: 4.5 hours (0.45 o/o)

Actual Operating Time/Scheduled Operating Time 99.51 o/o

Breakdown of Emergency Maintenance Time:

Main frame of computer: 1 hour (solder short between pins in inter-chassis socket)

1607 magnetic tape unit: 4.5 hours (tape wrapped up on pinch roller)

E. Neff

3.4 Artificial Intelligence

3.4.1 Simple Game Playing

The preceding progress report described a computer program which enables the computer to play a simple game against a human opponent. This program demonstrated that the machine could play "correctly" (i.e., according to the rules) and, more importantly, could learn to play a respectable game against opponents of varying skill.

During this quarter a program has been written and tested which allows the computer to assume the role of both players. This means, for example, that the "machine learner" can play a number of games versus a machine opponent having a fixed level of skill. Or that both machine players can learn the game but use different learning techniques. The program is constructed to facilitate the substitution of various learning techniques. Through a peculiarity of the game it is possible at any point in the learning process to determine objectively the level of skill of a machine player, thus allowing various learning techniques to be compared easily.

3.4.2 Electronic Music

In recent months computer generation of musical sounds has ceased to be merely a novelty and has become a serious research effort (at, among other places, Bell Telephone Laboratories). There are many reasons for this, among them the fact that computers can generate sounds difficult or impossible for human musicians to create and can sight read perfectly. This latter feature allows a composer to try complex musical ideas without allowing a long rehearsal time for musicians.

The multiple accumulator design of the CSX-1 computer lends itself very well to the real-time generation of multi-voice music. Circuits have now been constructed which extend this facility so that the composer has control of pitch, duration and loudness of individual notes (programmable), attack and timbre characteristics of the various voices (switchable).

This work was done jointly with Dr. L. A. Hiller and Robert Baker, both of the Music Department.

J. Divilbiss

3.5 Air Traffic Control Studies

The second of two reports entitled Automatic Air Traffic Control will be published in March. Part II, CSL Report R-146, is sub-titled "An Experimental Control Logic." An abstract of the second report follows.

The Work in automatic air traffic control conducted at CSL has consisted of three phases: 1) design of an automatic control system, 2) design of an experimental control philosophy, and 3) evaluation of the control philosophy in real-time simulation. This report, i.e. Part II, describes the experimental control philosophy and the results of the simulation. The simulation was done on the Cornfield System which consists of a special purpose tracking computer (TASC) and a general purpose digital computer (ILLIAC) connected together.

Three main control programs have been written as follows.

1) PILOT simulates manual control of a square en route area 128 miles on each side with sixteen airports.

2) PICON (for PILOT-CONTROL) simulates automatic control of en route, approach and terminal sequencing areas. En route area is square, 128 miles on each side and contains one airport with associated approach area (30 mile radius).

3) PICON-ER (for PILOT CONTROL EN ROUTE) simulates automatic control of en route and approach areas. Control area is square, 512 miles on each side with up to sixteen airports and approach areas.

In all cases, simulated traffic is made up of 4 different types of aircraft ranging in speed from 131 mph cruise to 542 mph cruise. The method of steering is radar vectoring via digital data link. Cornfield System computation speeds have limited system capacity to 25 controlled flights and shortage of memory space has limited the number and complexity of the rules used to control traffic. It was also necessary to assume zero winds aloft, well behaved air traffic, and one altitude. The Cornfield System limitations are shown to be non-existent in the system described in Part I.

In the automatic control programs, the control philosophy in en route phase of flight consists of navigation and conflict resolution. Navigation consists of steering traffic directly toward respective destinations and conflict resolution consists of steering to avoid conflicts by a defined margin. In extreme cases, conflicts are resolved by resorting to a standard 1 minute holding pattern. In approach area, navigation is the same as described above but the only method of resolving conflicts is by holding. In terminal sequencing, a passive form of conflict avoidance is employed and traffic is steered only to provide defined spacings in landing.

L. Kypta

4. SYSTEM THEORY

M. E. Van Valkenburg
J. B. Cruz, Jr.
H. Chang
W. K. Chen
D. Diamond
J. Elsey
S. J. Kahne
J. Kruus
W. W. Lichtenberger
W. Mayeda
T. Murata
R. Narayanasamy
W. R. Perkins
J. Resh
S. Seshu
D. Snyder
M. Sobral, Jr.

4.1 Introduction

This group is concerned with three general areas of research. One area is automatic control theory. For the most part, attention is focused on various aspects of optimum and adaptive control systems. Another area of research is circuit theory including linear graph theory and computer methods in network design. Applications of linear graph theory to communication nets and switching theory are being studied. A third area of research is sequential machine theory. Presently, work is in progress on algorithmic design of sequential switching circuits, automata theory, and self-repair.

4.2 A Method of Control Law Generation Using Sequential Phase Space Constraints

Progress during the last quarter may be broken up into three parts. These parts are listed below with a brief description of the work done.

4.2.1 Generalization of Constraint Mapping Technique

As reported earlier[1,2,3] a constraint mapping technique has been devised for mapping state space constraints into the control space and taking the intersection of this subset with the control space subset (given as part of the problem statement) to find an admissible set of controls. It was also shown[3] that the subspace so determined necessarily contained all admissible controls. However, it was not sufficient to use a control from this subspace. Further it was shown that one could define a region of the control space which did contain exactly all admissible controls but that this region was a function of the present state of the system. After further study it turned out that this procedure could be applied to a much wider class of systems than originally thought. The class to which the technique applies is called the class of

---

1 Quarterly Progress Report, June, July, Aug., 1962.

2 Quarterly Progress Report, Sept., Oct., Nov., 1962.

3 R-155, "A Constraint Mapping Technique for System Optimization," Nov. 5, 1962.

invertible systems. Two subclasses are defined. A careful definition of this class of systems follows:

4.2.2 Definition of Invertible Systems

If $$\dot{\underset{\sim}{x}}(t) = \underset{\sim}{f}[\underset{\sim}{x}(t), \underset{\sim}{u}(t), t] \qquad (1')$$

we say that (1') is invertible if there exists an analytical expression for $\underset{\sim}{g}$ such that

$$\underset{\sim}{u}(t) = \underset{\sim}{g}[\dot{\underset{\sim}{x}}(t), \underset{\sim}{x}(t), t]. \qquad (2')$$

Since we are dealing with a problem of numerical solution of optimization problems, we immediately turn our attention to the discrete version of (1') and (2') namely

$$\underset{\sim}{x}(K+\Delta) = \underset{\sim}{f}[\underset{\sim}{x}(K), \underset{\sim}{u}(K), K, \Delta] \qquad (1)$$

and

$$\underset{\sim}{u}(K) = \underset{\sim}{f}[\underset{\sim}{x}(K+\Delta), \underset{\sim}{x}(K), K, \Delta]. \qquad (2)$$

Two general classes of invertible systems may be defined as follows.

A. Class α invertible systems

This class is made up of two subclasses:

a) Class α_1 (multi-linear) invertible systems:

$$\underset{\sim}{x}(K+\Delta) = \underset{\sim}{f}[\underset{\sim}{x}(K),K,\Delta] + B[\underset{\sim}{x}(K),K,\Delta]\ \underset{\sim}{h}[\underset{\sim}{u}(K)] \qquad (3)$$

where

$B[\underset{\sim}{x}(K),K,\Delta]$ is a n $\times$ n matrix with the typical element

$$b_{ij} = b_{ij}[\underset{\sim}{x}(K),K,\Delta], \qquad (4)$$

$\underset{\sim}{h}$ is an n-vector with the typical element

$$h_i = \sum_{j=1}^{n} a_{ij}u_j(K). \qquad (5)$$

b) Class α_2 (non-linear, non interacting) invertible systems:

$$\underset{\sim}{x}(K+\Delta) = \underset{\sim}{f}[\underset{\sim}{x}(K),K,\Delta] + B[\underset{\sim}{x}(K),K,\Delta]\ H[\underset{\sim}{u}(K)],$$

where B is as in (4) above and H is an n $\times$ n diagonal matrix with the following typical elements:

$$h_{ij} = \begin{cases} h_{ii}[u_i(K)], & i=j, \\ 0, & i \neq j. \end{cases} \quad (7)$$

B. Class β invertible systems: This class contains all invertible systems not contained in class α.

Introduction of this class of systems leads to a new problem statement for this investigation. The new problem statement follows:

4.2.3 Statement of the Problem

Given the following class α invertible system

$$\dot{\underset{\sim}{x}}(t) = \underset{\sim}{f}[\underset{\sim}{x}(t),t] + B[\underset{\sim}{x}(t),t]\, \underset{\sim}{h}[\underset{\sim}{u}(t)], \quad (8)$$

determine $\underset{\sim}{u}(t)$ such that

$$F[\underset{\sim}{x}(t), \underset{\sim}{u}(t),t] \quad \text{is minimized, and} \quad (9)$$

$$\underset{\sim}{x}^-(t) \leq \underset{\sim}{x}(t) \leq \underset{\sim}{x}^+(t), \text{ and} \quad (10)$$

$$\underset{\sim}{u}^-(t) \leq \underset{\sim}{u}(t) < \underset{\sim}{u}^+(t). \quad (11)$$

The terms are identified as follows:

$\underset{\sim}{x}(t)$	(n-dimensional) state vector,
$\underset{\sim}{x}^{\pm}(t)$	(n-dimensional) state space constraints,
$\underset{\sim}{u}(t)$	(m-dimensional) control vector,
$\underset{\sim}{u}^{\pm}(t)$	(m-dimensional) control space constraints,
F	performance index,
$\underset{\sim}{f}$	(n-dimensional) system vector,
B	(n × n dimensional) interaction matrix.

The control vector $\underset{\sim}{u}^o(t)$ which satisfies (9) subject to (8), (10), (11), is called the globally optimum control vector. If $\underset{\sim}{u}'(t)$ is such, for all $\delta\underset{\sim}{u}(t)$ a small perturbation in $\underset{\sim}{u}(t)$, that

$$F[\underset{\sim}{x}'(t), \underset{\sim}{u}'(t),t] < F[\underset{\sim}{x}'(t) + \delta\underset{\sim}{x}(t), \underset{\sim}{u}'(t) + \delta\underset{\sim}{u}(t),t],$$

then $\underset{\sim}{u}'(t)$ is a locally optimum control vector.

The techniques of this study determine a locally optimum control vector. To find the globally optimum control vector, we simply select the "best" locally optimum one. By this is meant that if ${}^{1}\underset{\sim}{u}(t)$ ${}^{2}\underset{\sim}{u}(t),\ldots,{}^{K}\underset{\sim}{u}(t)$ are locally optimal, then if there exists j such that, for all $i \neq j$,

$$F[{}^{j}\underset{\sim}{x}(t),\ {}^{j}\underset{\sim}{u}(t),t] < F[{}^{i}\underset{\sim}{x}(t),\ {}^{i}\underset{\sim}{u}(t),t].$$

We call ${}^{j}\underset{\sim}{u}(t)$ the globally optimal control vector. Since the number of locally optimal control vectors may be very large, generally, as in this work, one is satisfied to find a locally optimal control vector.

4.2.4 Computer Results

The computer programs which mechanize the numerical procedure developed in this investigation have been written and several examples run. The results are encouraging and have pointed the way to several minor changes in the optimization procedure. The changes were made and appear to verify the theoretical predictions of behavior of the method.

4.2.5 Preparation of Final Report

This project will be completed during the coming quarter. A final report has been initiated and about one quarter of it has been completely written. The title of this report will be "On Direct Fixed-Time Optimization of Invertible Systems." The fixed-time designation indicates that the control period is to be assumed fixed at the outset of the optimization procedure.

S. J. Kahne

4.3 Linear Multivariable Systems - Stability Considerations

A method to design optimum, stable controllers was given in the previous progress report. During this quarter, the system stability with respect to plant parameter variations was considered. The necessary and sufficient conditions for the stability of linear multivariable systems are under investigation.

R. Narayanasamy

4.4 Control Optimization with Multirange Constraints

The formulation of a new control problem was carried out during the past quarter. We consider a sequence of vector differential equations defining a dynamic process over various ranges in time. The sequence of state vectors may have some components which are common. We impose control vector and state vector integrals constraints over the various ranges. The performance index may involve a sequence of state vectors and a sequence of control vectors. A problem under investigation is to choose a sequence of control vectors which satisfies the constraints and the sequence of process differential equations, and which optimizes the performance index. We have reformulated the problem into one which involves multiterminal constraints rather than integral constraints.

J. B. Cruz, Jr.
S. J. Kahne

4.5 Sensitivity Studies for Nonlinear Feedback Systems

This is a new project initiated during the last quarter. The main objective is to study the effect of parameter variations in nonlinear plants. The basic question is to determine under what conditions feedback compensation is superior to cascade or open loop compensation, from the point of view of plant parameters variation. Block diagram models for the effect of plant parameters variations on the complete input-output characteristics have been obtained using the theory of nonlinear operators.

J. B. Cruz, Jr.
W. R. Perkins

4.6 Design of Ladder Filters by Computer

In 1961, C. A. Desoer[4] and others used a steepest descent method to minimize the sum squared difference between the magnitude functions of ideal and lossy networks for a set of frequencies. The networks considered are passive, ladder filters with time invariant elements. We plan to use the Taylor Series approach[5] which does not deal directly with minimizing the norm of an error but minimizes the sum of the squares of the difference between the ideal response and its linear approximation at the sampled points (or discrete frequencies). Experience[6] has shown that this approach is powerful when the function depends linearly on system parameters (e.g., network elements). If the function is not linearly dependent on system parameters, then a modification such as a relaxation method will be needed.

---

4 C. A. Desoer and S. K. Mitra, "Design of Lossy Filters by Digital Computers," IRE Trans. on Circuit Theory, vol. CT-9, pp. 192-201; Sept., 1961.

5 M. R. Aaron, "The Use of Least Squares in System Design," IRE Trans. on Circuit Theory, vol. CT-3, pp. 224-231; Dec., 1956.

6 H. Sinozaki, T. Murata and others, "Application of Digital Computer to Network Design," (in Japanese), Convention Record of Japanese Professional Research Committee on Network Theory, July, 1962.

The method to be studied requires the evaluation of the magnitude at a set of discrete frequencies. A preliminary version of this method has been programmed in FORTRAN for the CDC 1604. Results will be reported later.

Tadao Murata

4.7 Contact Network Synthesis

The computer program for synthesizing absolutely minimal contact networks for given Boolean functions is now practically complete and is expected to be in production very soon. It is hoped that the program will provide answers to some outstanding academic questions.

W. Mayeda
S. Seshu

4.8 Automata Theory

The literature survey undertaken earlier in the year is now complete and a report together with an annotated bibliography is being issued.

H. Y. Chang

4.9 Self-Diagnosis

A new project was initiated during the last quarter on the diagnosis of sequential machines. The general problem has been discussed by Seshu and Freeman. The primary tool of this study is a computer program. This program is currently being written for the CDC 1604 computer. This project has four major objectives:

1. Understanding methods of programming a computer to execute decision processes effectively and efficiently (heuristic programming).

2. Study the problem of interconnecting a set of solutions obtained for the pieces of a computer to produce a set of system diagnostics.

3. Study the problem of organizing a digital computer to facilitate self-diagnosis.

4. Provide the basic tool for several future investigations (Ph.D. theses) in this area.

The "working core" of the program, comprising 4000 machine language instructions, is now complete. The final program is expected to be about 10000 instructions for the CDC 1604 computer. Plans are under way for encoding the logic of the CSX-1 computer so that the study can utilize a "real system" as an example.

S. Seshu

4.10 Design of Sequential Switching Circuits

Early computer results for algorithmically designing sequential switching circuits from input-output specifications showed that an unreasonably large number of input-output entries were necessary to completely specify some simple problems. A more feasible specification appears in most cases to be a flow table. The procedures developed for designing sequential circuits from input-output sequences were modified so as to provide for a flow table problem specification. A machine language program for the CDC 1604 computer was written to verify the capabilities of the method. Results as of this date indicate that the procedure compares fairly well with other procedures, notably that developed by Huffman. The number of secondary variables required for realization varies from 1.0 to about 1.7 times the number needed for a Huffman realization in the examples already worked, but time estimates indicate that this procedure is several orders of magnitude faster than that of Huffman. One example was worked in which varying quantities of the data were available, the procedure gave a realization requiring only 1.75 times as many secondary variables as that obtained by Huffman's procedure. (Huffman's procedure requires all of the data to be available.) With 15 o/o of the data available, only 1.25 times as many secondary variables were needed.

Other examples are being prepared and some small changes are being made in the program to provide a better analysis of the capabilities of the procedure.

J. Elsey

4.11 Self-Repair

A program has been written for the CDC 1604 computer to simulate various organizations of systems with repair and replacement. It is proposed to expand the program to simulate self-repairing systems composed of several kinds of basic components. By injecting random failures, it will then be possible to evaluate the efficiency of the different organizations in increasing system lifetime at the cost of greater complexity and an increased number of repairs.

In its present state of development, the program is used to simulate systems consisting of only one kind of basic machine. Three or more of these work in parallel with failures being detected by a majority organ. When a failure is detected, the failed machine is replaced by a stand-by (which may also have failed while waiting to be put into operation). A time of at least T_c is required to repair a failed machine and/or prepare the next stand-by machine for operation. T_c may be specified by an arbitrary probability distribution.

The results of simulating these systems are being compared to analytical calculations of system reliability in an attempt to develop reliable and workable exact methods of calculating the reliability or in checking the validity of any approximations made. In the case of the simplest system ($T_c = \infty$) a solution has been found which agrees excellently with the simulation results. The program has already been found extremely valuable in indicating errors in the calculations. It is expected that its usefulness will even increase as more complex systems are studied.

J. Kruus

4.12 Linear Graph Theory

A digital computer program for testing the realizability of a given matrix as the fundamental cut set matrix of a non-oriented graph has just been completed. This is to be combined with Seshu's routine, whose purpose is to generate all switching functions which are equivalent to a given switching function. Thus it will be just a matter of time until minimum contact networks are found for several switching functions whose minimum realizations have been unknown up to the present.

W. Mayeda

4.13 Communication Nets

If there exists one communication net which has a given matrix T as its terminal capacity matrix then in general there exist uncountably many such nets. This immense set of realizations of T can be partitioned into a finite number of equivalence classes. Among these equivalence classes for a particular T there may be one which is distinguished from the others by virtue of having a certain property. For some time now I have been trying to prove that, in fact, this special class is present for any realizable T. I recently found an algorithm for obtaining from any realization of T a member of the special class if it is nonempty but, unfortunately, this has not yet shed any light upon the general question of the existence of this class.

J. Resh

5. PLATO

D. Bitzer
R. A. Avner
R. Blomme
P. G. Braunfeld
O. R. Brown, Jr.
D. Diamond
J. Easley
E. R. Lyman
L. Morgan
M. Secrest
B. W. Voth
R. Willson
H. Wills

5.1 Introduction

The purpose of the PLATO project is to develop an automatic teaching system for tutoring simultaneously a large number of students in a variety of subjects. The central control element of the teaching system is a general purpose digital computer. The PLATO system differs from most teaching systems in that a single high speed digital computer is used to control all student stations. Thus, it can bring to bear the power of a large digital computer in teaching each student.

5.2 Physiological Measurements

By the end of January, electrocardiogram data had been collected on nine subjects who worked completely through the lesson program known as CHAOS. Further work is required on equipment for recording physiological data during a lesson, but this work has been temporarily discontinued in order to concentrate on analysis of data already acquired, preparation of new instructional materials, and a new project (DOPA) to be described shortly.

Several different modes of data analysis were partially carried through in order to discover which mode of presentation maximizes the clarity of relationships between stimulus and response data, on the one hand, and heart rate on the other. It was finally decided to represent heart rate as number of beats per tenth of a minute. Heart rate was then plotted as a graph on the same sheet as a time response graph for keyboard data. One of these graphs is shown in Figure 5.1. Graphs of keyboard data have made it possible to analyze more easily the type of intellectual activity being carried on by the student, at least for the lesson time covered by keyboard activity. The time scale was divided into intervals representing discovery, rediscovery, false discovery, routine calculations, and indeterminate activity. Work is now underway in averaging heart rate for each of these different types of time intervals. Preliminary examination of mean heart rate seems to show a reliable difference in the level

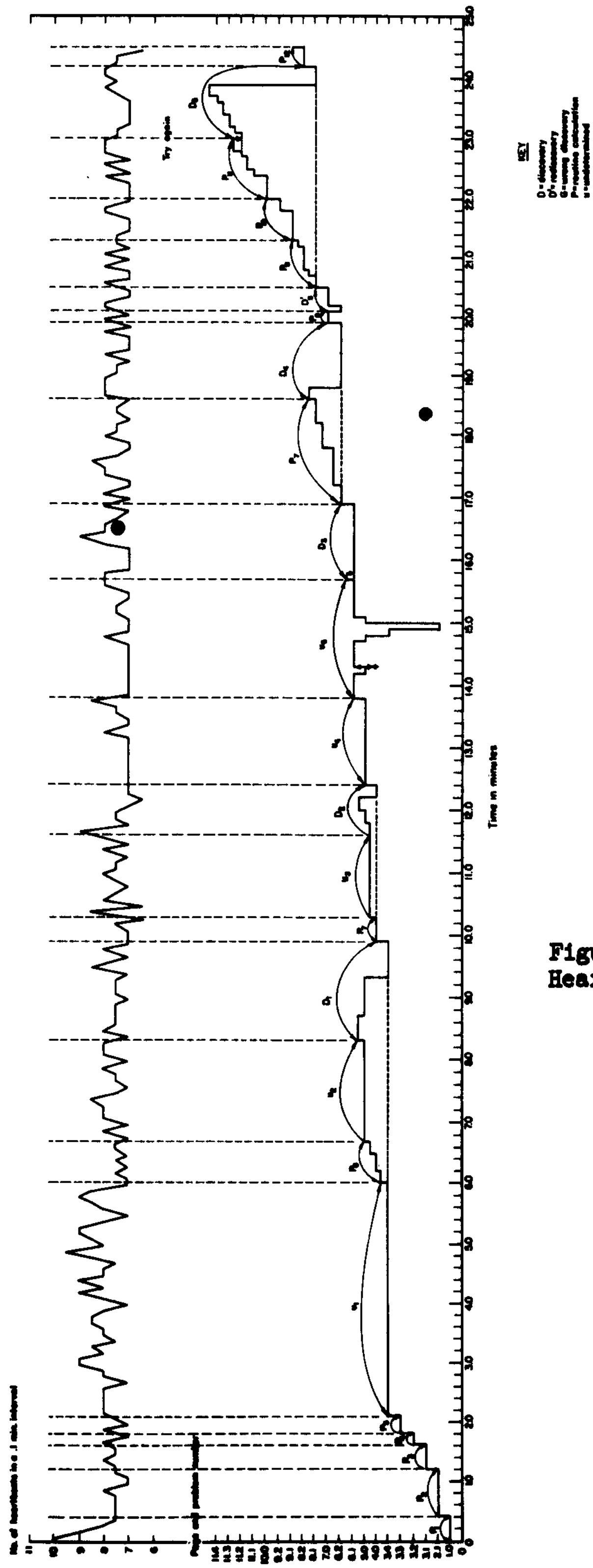

Figure 5.1.
Heart Rate Chart.

of activity between discovery periods and routine calculations. More definite conclusions await completion of computation of variances.

The original CHAOS program permits students to discover patterns in numerical sequences. Work is now underway preparing a program which will include patterns in geometrical arrays, such as the triangular numbers, and which will permit study of the extent to which patterns so discovered can be transferred to other problems and also used in combinations in a kind of derivation. Programming of this material will be carried out in such a way as to minimize the periods in which the students' activity is indeterminate.

A new lesson program has been launched to develop a Demonstration of Proofs in Algebra (DOPA) to be performed by a student in the PLATO lab mode. The specifications for the DOPA teacher have been worked out in great detail for this program, pages have been typed for photographing on slides, and the constant list has been prepared. Preparation of the DOPA parameters for use with PLATO LAB is now under way. In order to detect the weaknesses remaining in this teaching logic, it is planned to test this program with University High School students who have completed a unit in high school algebra which treated such proofs. It is also planned that a program for teaching proofs of this form will be completed for use with teachers attending the NSF Summer Institute this summer.

The general idea of the teaching for DOPA is that the computer will print on the blackboard each line of a proof once a student has supplied the principle, the substitutions, and essential copying instructions which justify that line as a conclusion from a preceding line. That is, the machine supplies the logical rules and refuses to act in violation of them; the student must supply the strategy or heuristics necessary to arrive at the desired conclusion. The major problem in this project has been to eliminate the possibility of drawing invalid conclusions. A period of testing this program will be needed, however, in order to insure that no loopholes have been overlooked. It is also expected that students working on this program will provide interesting data on the psychology of heuristic thinking and strategy, and that physiological measures such as heart rate will show interesting changes as the student moves from analysis to synthesis in the development of a proof.

It is hoped that this demonstration program will be a stimulus to other writers to prepare a sequence of such lessons which will develop the ability to create proofs by students who have not had previous experience of this kind.

J. A. Easley, Jr.

5.3 PLATO Laboratory

The PLATO Laboratory program was completed in December and a demonstration lesson using applications of Archimedes principle was written. On January first, the ILLIAC computer was no longer available and so the PLATO II equipment was modified for use with the 1604 computer.

The PLATO Laboratory program offers possibilities for "teachers" different from the PLATO II teacher. To demonstrate its varied use, two "teachers" have been in the process of preparation during the last half of this quarter. One of these, DOPA, is reported by members of the UICSM project in another part of the PLATO progress report. Almost completed is a program for Dr. Richard Suchman and his associates for use in the scientific inquiry study which he is carrying on with 11 and 12 year old students. The program allows a student to see a brief film demonstrating the properties of a bimetal strip and then to follow his own path, via PLATO Laboratory through questions, answers, and simulated experiments until he arrives at conclusions about the basic principles involved in the bimetal strip experiment. A record of the student's pattern of discovery is kept by the computer and is provided at the end of each student's lesson. The PLATO Laboratory program allows progress back and forth through the lesson material via linked modes. The linking of the modes and the calculations performed in each mode are specified by the parameters for each lesson.

The PLATO Laboratory program with its versatile linked mode construction has suggested the possibility of a very general master program for PLATO which will allow non-computer trained persons to write their own "teachers" for whatever kinds of lessons they desire. The users will be able to write the teachers in a pseudo language which the computer will then be able to read, compile and assemble into the particular "teacher" program. Work has now been started on the general program and we plan to have it completed in the next quarter.

D. L. Bitzer
E. R. Lyman

5.4 PLATO III Computer Program

In the Quarterly Progress Report for June 1962 a PLATO III program for use with the CDC 1604 was outlined. During the past quarter a substantial part of this program was coded and it is expected that the complete program will be ready for checking with the new PLATO III equipment by April, 1963.

While coding of the program was in progress, we also considered what lesson material would be apt for use with the new program, particularly for demonstrating its more unusual and powerful features. In preparation are a lesson in astronomical measurement for grade school children, and an exposition of the elements of permutation groups.

P. Braunfeld
L. Morgan

5.5 PLATO III System Equipment

PLATO III, the system now being developed, differs from PLATO I and PLATO II in that a maximum of 32 students (rather than only two students) can be taught concurrently.[1] In addition, the PLATO III system will have greater flexibility due to an increased slide capacity and incorporation of a selective erase for the blackboard. A block diagram showing the organization of the PLATO III equipment is shown in Figure 5.2.

5.5.1 Equipment Shared by all Students

Input-Output Interface. This segment of the PLATO III equipment is designed to act as the buffer between the 32 student stations and one input-output channel of the CDC 1604 or the CSL CSX-1.

The modules required for operation with the CDC-1604 are nearing completion and should be ready for testing as a unit early in the next quarter. Most of the modules will plug into a specially adapted rack (which is also nearing completion at this time), while two driver modules are being located near the computer to allow semi-remote operation (the student stations will be two floors away from the computers). Operation will start with two student stations, with additional stations added two at a time as completed.

Slide Scanner (electronic book). The present slide scanner in use with the PLATO II system has been equipped with new photo-multiplier pre-amps

---

[1] Bitzer, Braunfeld, Lichtenberger: PLATO II: A Multiple-Student, Computer-Controlled, Automated Teaching Device. CSL Report I-109, October 1961.

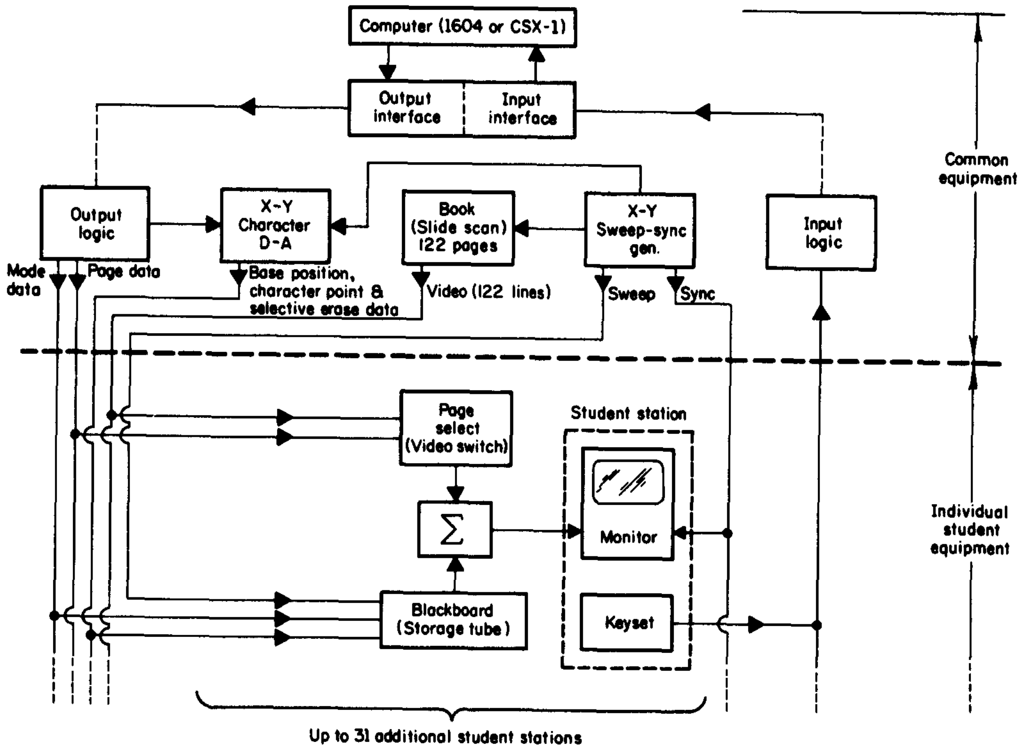

Figure 5.2. Equipment Organization Chart.

which have completely eliminated a tendency for weak oscillations to appear on certain selected slides. The present slide selector along with a second duplicate slide selector will be made ready for use with the PLATO III system during the coming quarter.

X-Y Character, Sweep, and Sweep-sync Generators. Prototype character D-A, TV sweep, and sweep sync circuitry providing for write, read, blanking, and sync signals common for all student stations is nearing completion. It is expected that performance evaluation and if necessary, further development of the circuitry will be undertaken in the coming quarter. In addition, construction of prototype X-Y circuitry providing for selective erase will be undertaken.

5.5.2 Individual Student Equipment

Storage Tube Control Logic. Cards for one student station have been completed and installed in the storage tube module. Testing has not yet been completed. The cards for another student station have been started.

Storage Tube Circuitry (electronic blackboard). Final layout, fabrication, and checkout of a prototype, hybrid-vacuum tube-transistor storage tube pre-amplifier was begun. The performance of the new amplifier appears satisfactory.

Performance evaluation of a hybrid vacuum tube-transistor deflection amplifier required for storage tube beam deflection was also undertaken this quarter. Early results indicate adequate recovery and stability characteristics.

Keysets. Four keyboards have been obtained from Teletype Corporation. The circuitry designed and constructed to allow their operation with the PLATO III system has been completed. Minor modifications to the keyboards themselves must still be made.

D. Diamond
B. Voth

5.6 Plasma Storage Tube

The purpose of developing a plasma storage tube is to find a less expensive replacement for the present storage tube system.

During the last quarter experiments have shown the feasibility of switching the grid structure using an R.F. initiated plasma to establish a D.C. path. The intersection of the horizontal and vertical D.C. paths select the specified spot to be initiated on the "screen" and raise the potential there so that a smaller R.F. signal may initiate and subsequently sustain this discharge. The experiment has been performed at ten megacycles using neon discharge bulbs to similate the grid structure.

A four by four array (sixteen spots) has been constructed but difficulties in obtaining ten megacycle transformers and neon discharge bulbs with nearly uniform initiating potentials prevented testing the array in time for this report.

R. H. Willson

6. VACUUM INSTRUMENTATION

E. Alpert
W. C. Prothe
Donald Lee
Wil Schuemann
Jose L. de Segovia
Harry Tomaschke

6.1 Sticking Probability of N_2 on Molybdenum

During this quarter the sticking probability of N_2 on molybdenum was again measured. In previous experiments it was observed that when N_2 was introduced into a system the sticking probability would increase with coverage and then fall. This unusual result could be explained by a substitutional adsorption involving CO. The vacuum system being used to repeat the previous experiments differs from the previous system only in that an omegatron has been added. This work is still in progress.

6.2 Anomalous Behavior of Ionization Gauges

The investigation into anomalously high collector currents in ionization vacuum gauges mentioned in the last progress report has been continued. We are convinced that under certain circumstances the ionizing electrons, when they are collected on the grid surface, cause the formation of ions. A fraction of these surface ions are collected and hence can give rise to abnormally high collector currents. We have definitely shown that the double collector gauges of Redhead and Lee do not give meaningful readings when surface ionization currents are comparable to volume ionization currents. The probable maximum error introduced by surface ionization when a standard Bayard-Alpert gauge is running at 10 ma is not sufficient to reduce the usefulness of the gauge for the vast majority of applications. This work is also being continued.

6.3 Photo Suppressor Gauge Tests

We are continuing to use the photo current suppressor gauges mentioned in four previous progress reports. Our typical vacuum system base pressures have been shown to be 1×10^{-11} Torr without any cryogenic pumping. Our confidence in the gauge is increasing and it has already proved to be a valuable research tool in the investigation of the anomalous ion current mentioned above.

W. Schuemann
Jose de Segovia

7. PLASMA PHYSICS

M. Raether
J. K. Aggarwal
A. Barger
W. Carr
C. Chen
J. Crowder
J. Harris
B. Hicks
T. Lie
C. Mendel
H. G. Slottow
J. B. Tsui
T. Utsumi

7.1 The Boltzmann Equation for a Shock Wave

The quarter has been occupied both with tests of the 1604 program that make use of its high speed and with the development of additional test programs.

A series of calculations was made for a Mach number of 1.341 for samples of two sizes, with and without the moment correction. Instability of the type found in the ILLIAC calculations for this Mach number have disappeared but the fluctuations still are very large. The moment calculations near the cold boundary sometimes produced another type of instability. The program was therefore modified so that moment corrections are automatically omitted when these would produce sizeable distortions of the velocity distribution function.

Even though calculations of shock structure appeared to be successful in the previous quarter for the higher Mach number of 3.17, two unsatisfactory features of the overall method remain: the large fluctuations for the low Mach number case and an apparent bias in the calculation of the collision integral. Each difficulty suggests the need for making a close study of the calculation of the collision integral, (a-bf), a need that is obvious in the case of the apparently biased results, but which requires a little explanation in the case of the low Mach number calculations. For low enough Mach numbers, the Monte Carlo method may be expected to fail, because the collision integral must then be calculated as a small difference of two quantities, each of which is subject to statistical fluctuations. (Nordsieck's version of the Monte Carlo method cancels part of these fluctuations.) Finding the lower limit of the Mach number for which the Nordsieck calculation of shock structure is possible requires examination of the accuracy of the calculation of each of the two parts of the collision integral. Note that a bias in the calculation of the collision integral near the boundaries might disturb the calculation more for low Mach numbers than for high Mach numbers, for in the later case it may, in effect, distort only the distance scale within the shock.

In order that suitable tools to study the collision integral calculation would be available, the second half of the quarter was devoted to writing and testing new and modified routines (ANLTABF, DFTAB, PSTAB, IOSLET, NUN, and NUP) and incorporating them into the main program. In various combinations these new routines make possible the following studies:

a) Calculation of exact values of $a(\underset{\sim}{v}) = a_n(\underset{\sim}{v})$ for both the cold and hot equilibrium distributions;

b) Isoline displays via ISOLET of values of a, a_n, a-bf, a-a_n, $\psi(a/a_n)$ as functions of $\underset{\sim}{v}$;

c) Calculation of $\int X(\underset{\sim}{v})d\underset{\sim}{v}$ and $\int X(\underset{\sim}{v})v_{xa}^{-1}\,d\underset{\sim}{v}$ where $X(\underset{\sim}{v})$ is alternatively $a(\underset{\sim}{v})$ and (a-bf).

These integrals represent such physically interesting quantities as collision rates and density gradients, and in addition are useful in monitoring calculation of the collision integral. The density gradient will also be necessary in the future in an improved method of integration of the Boltzmann equation itself. Preliminary calculations with these two tools tends to confirm the bias in the Monte Carlo calculation of the collision integral and suggest that possibly this bias is somewhat angle dependent. At least part of the next quarter will be devoted to searching for the origin of these apparent biases. Monte Carlo calculations of the parts of the collision integral are feasible on the CDC 1604 for 40,000 or more collisions, making possible valuable studies of convergence as a function of sample size.

A report entitled "Numerical Studies of Strong Shock Waves, Part II: Results of ILLIAC Calculations." was prepared in October for internal use. This paper, with small modifications, was submitted in January for reproduction as CSL Report I-117.

J. K. Aggarwal
B. L. Hicks

7.2 Momentum Transfer Cross Section of Electrons with Neon Atoms

In the preceding quarter, measurements on the temperature (200° - 600°K) dependence of the effective electron collision frequency in a decaying neon plasma have been completed. From these, one is able[1] to determine the energy dependence of the momentum transfer cross section of electrons with neon atoms. This result, together with the results obtained by other workers[2] at higher energies, is presented in Fig. 7.1. Fair agreement is noticed in the overlapping range of energies, except that the present experiment shows an apparent minimum in cross section in the neighborhood of 0.11 electron volts. Further theoretical study on this particular feature is proceeding since almost all semi-empirical theories[3,4,5] on the scattering cross sections of slow electrons with neon atoms predicted no such minimum. The apparent failures[6,7] in observing a Ramsauer effect by cross modulation[6,7] techniques can also be explained by the present experiment and analysis. A detailed report on this subject will be prepared in the near future.

C. L. Chen

1 Progress Report (Coordinated Science Laboratory) for September, October, November, 1962.

2 A. Gilardini and S. C. Brown, Phys. Rev. 105, 31 (1957).

3 B. Kivel, Phys. Rev. 116, 1484 (1959).

4 T. F. O'Malley, "Extrapolation of Electron-Rare Gas Atom Cross Sections to Zero Energy," Physics Department, New York University (1963). Unpublished.

5 B. L. Moiseiwitsch, "The Elastic Scattering of Zero Energy Electrons by the Inert Gases," Second International Conference on the Physics of Electronic and Atomic Collisions, University of Colorado, Boulder, Colorado, June 12-15, 1961. Published by W. A. Benjamin, Inc.

6 J. M. Anderson and L. Goldstein, Technical Report No. 7 AF19 (604) -- 524, Department of Electrical Engineering, University of Illinois, Urbana, Illinois (1955). Unpublished.

7 A. A. Dougal and L. Goldstein, Scientific Report No. 1 AFCRC-TN-57-388, Department of Electrical Engineering, University of Illinois, Urbana, Illinois (1957). Unpublished.

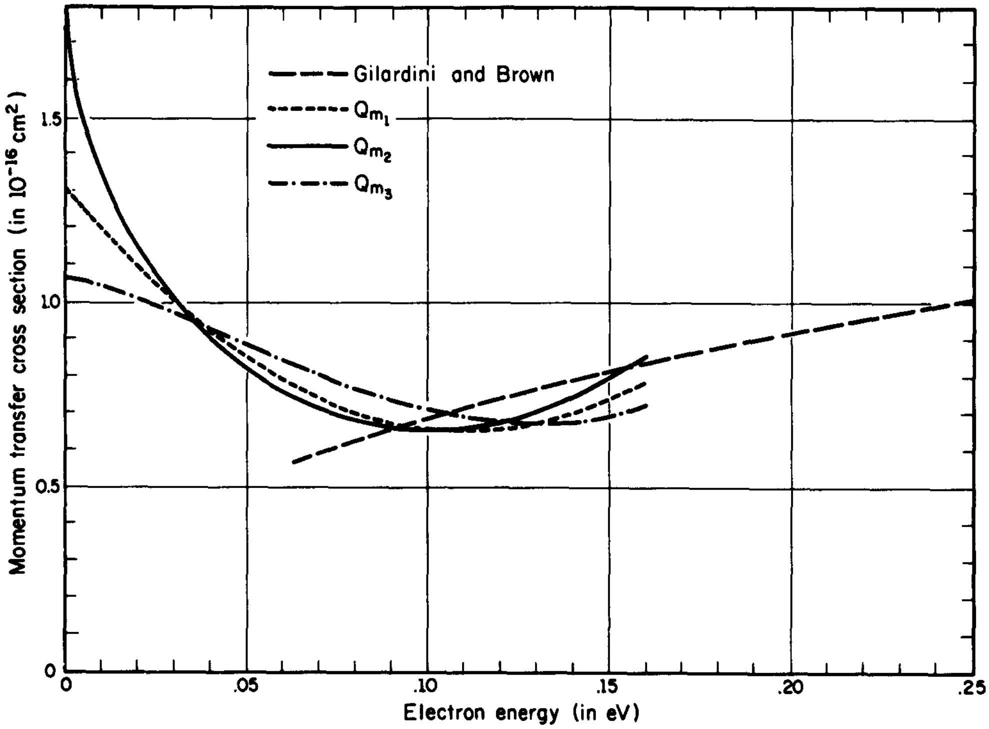

$Q_{m_1}(u) = 1.315 \times 10^{-16} - 1.19 \times 10^{-15} u + 5.37 \times 10^{-15} u^2 \text{ cm}^2$

$Q_{m_2}(u) = 1.854 \times 10^{-16} - 5.05 \times 10^{-16} u^{1/2} + 4.01 \times 10^{-15} u^2 \text{ cm}^2$

$Q_{m_3}(u) = 1.07 \times 10^{-16} - 2.127 \times 10^{-15} u^{3/2} + 9.92 \times 10^{-15} u^{5/2} \text{ cm}^2$

where u is electron energy in eV.

Figure 7.1. Momentum Transfer Cross Section.

7.3 Incoherent Scattering of Microwaves from a Plasma

The incoherent scattering of electromagnetic waves from plasmas is receiving much interest at the present time in conjunction with the backscatter of radio waves from the ionospheric F-layer[8] and the possibility of using laser beams for the diagnostics of high density plasmas. The theory of incoherent scattering of radiation from plasmas has been presented in a number of papers.[9,10,11,12] The characteristic features of the scattering cross section are sketched schematically in Fig. 7.2, where the cross section is plotted versus $\Delta\omega = |\omega - \omega_o|$, ω_o being the frequency of incidental radiation. The cross section has a first maximum in the neighborhood of kv_i (v_i is the mean ion velocity), a second much smaller maximum at kv_e (v_e is the mean electron velocity) which is omitted in the drawing, and a third sharp maximum at the plasma frequency. The absolute value of the total cross section is of the order r_o^2 (r_o is the classical electron radius).

We have made an attempt to detect the incoherent scattering of microwaves from a laboratory plasma. A schematic diagram of the apparatus is sketched in Fig. 7.3. A microwave signal of the order of 50 mw at 8855 mc. is propagated through the positive column of a DC-discharge housed in a waveguide. The discharge tube is filled with neon at 3 mm of Hg pressure and operated at a current of 15 ma. The electron density corresponds to a plasma frequency of $\omega_p/2\pi \sim 1500$ mc. The microwaves that have traversed the discharge are absorbed in a termination. Microwaves that are incoherently scattered in the backward direction pass the circulator and are mixed with a local oscillator such that the difference frequency falls into the passband of the IF-amplifier tuned to 30 mc, and of about 2 mc bandwidth. The microwave signal is modulated at 440 c/sec, by means of a gyroline, to permit detection with a polarity coincidence detector. Apart from incoherent backscattering, a considerable amount of coherent backscattering comes from the discharge tube and discontinuities in the waveguide system. A tuner is inserted before the termination which permits nulling this coherent part at the detector.

---

8 K. L. Bowles, Phys. Rev. Letters 1, 454 (1958).

9 J. P. Dougherty and D. T. Farley, Proc. Roy. Soc. A259, 79 (1960).

10 E. E. Salpeter, Phys. Rev. 120, 1528 (1960).

11 J. A. Fejer, Can. J. Phys. 38, 1114 (1960).

12 M. N. Rosenbluth and N. Rostoker, Phys. Fluids, 5, 776 (1962).

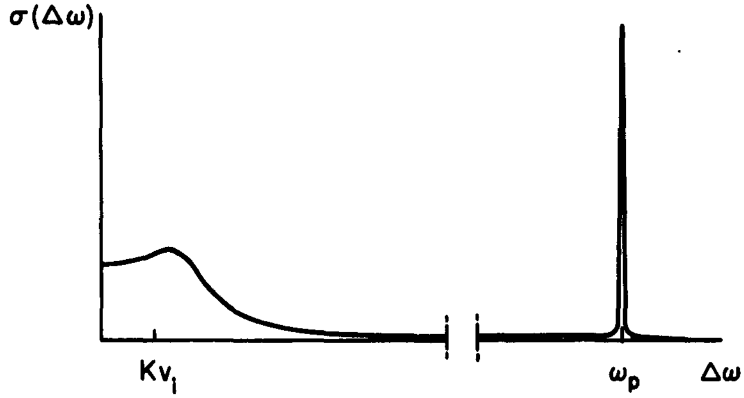

Figure 7.2. Cross Section for Incoherent Scattering of Electromagnetic Radiation from a Plasma (Schematic).

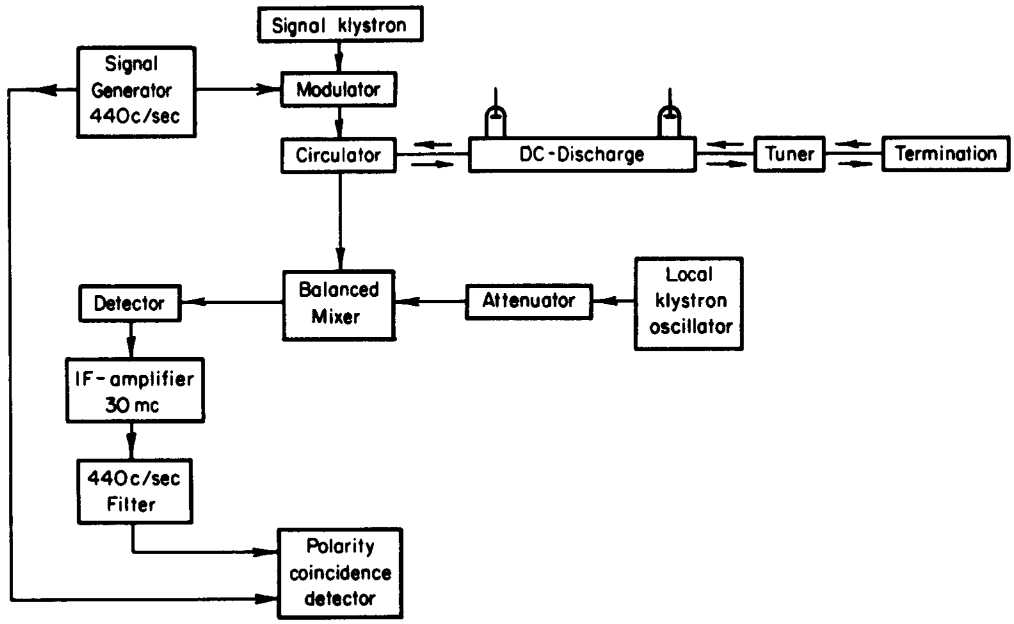

Figure 7.3. Block Diagram of Microwave Circuits.

Fig. 7.4 shows the preliminary results obtained. The output of the polarity coincidence detector is plotted versus the beat frequency. A slight signal increase is obtained in the neighborhood of $\omega_p + \omega_o$. Although integration times of one hour were used, the error is still considerable. More accurate measurements are needed before a comparison with the theory will be attempted. It is clear that the line width at the plasma frequency will be substantially increased over the theoretical value, due to the inhomogeneous electron density and the presence of electron-neutral collisions.

The greatest limitation in sensitivity is presently the noise of the IF-amplifier. The experiment is presently being modified in several ways to make more accurate measurement possible.

An attempt to look for the Doppler broadening of the central line was unsuccessful, due to the large density fluctuations in dc-discharges around zero frequency that overshadows the effect.

M. Raether
W. Carr

7.4 Plasma Delay Line

The crossed electric and magnetic fields in the plasma delay line not only control the perpendicular drift of charged particles, but they also constrain the particles from streaming along the electric field lines. Among the magnetic lines, however, there is no constraint, and in a practical device some means must be provided to contain the particles. In the plasma mode electrons are attracted by the ions, which, because of their greater intertia, diffuse more slowly[13]. In a circular electron device, focussing fields that do not vitiate equal time-of-flight conditions can be provided by hyperbolic electrodes.[14] In rectangular geometry, however, such focussing fields demand the introduction of conductors in the drift space.

One possible electrode configuration is shown in Fig. 7.5, which is a section of drift space perpendicular to the drift direction. The end plates are conductors set at fixed potentials, and the round dots represent cross sections of conductors that terminate regions of uniform electric field. The component of electric field, E_x, which, together with the magnetic field

---

[13] Coordinated Science Laboratory Progress Report Mar., April, May, 1962.

[14] Coordinated Science Laboratory Progress Report Sept., Oct., Nov., 1962.

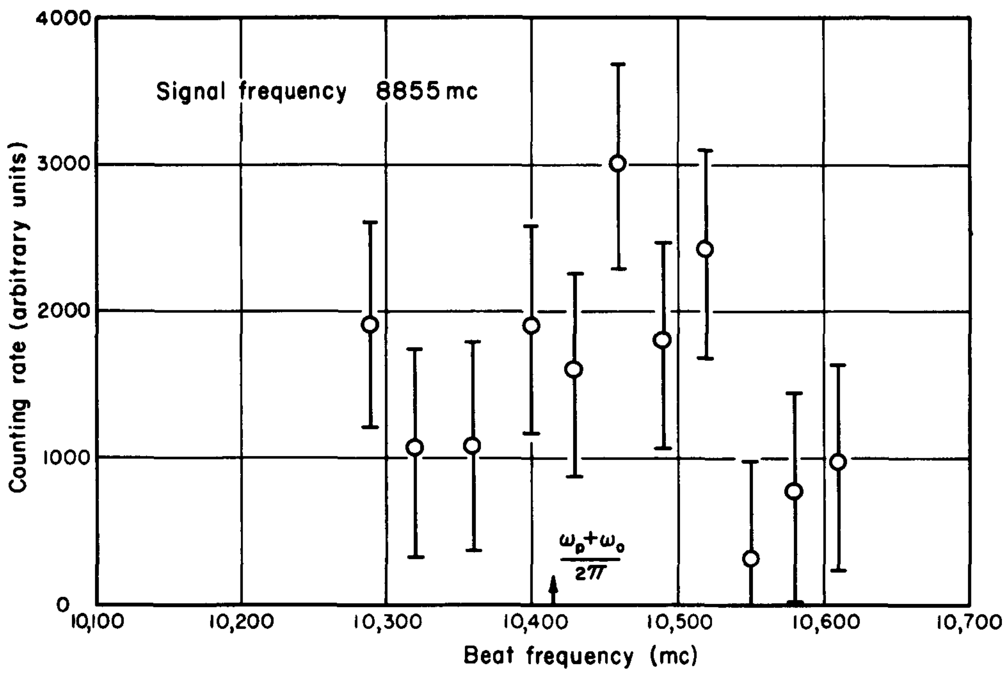

Figure 7.4. Incoherent Scattering of Microwaves from a Plasma.

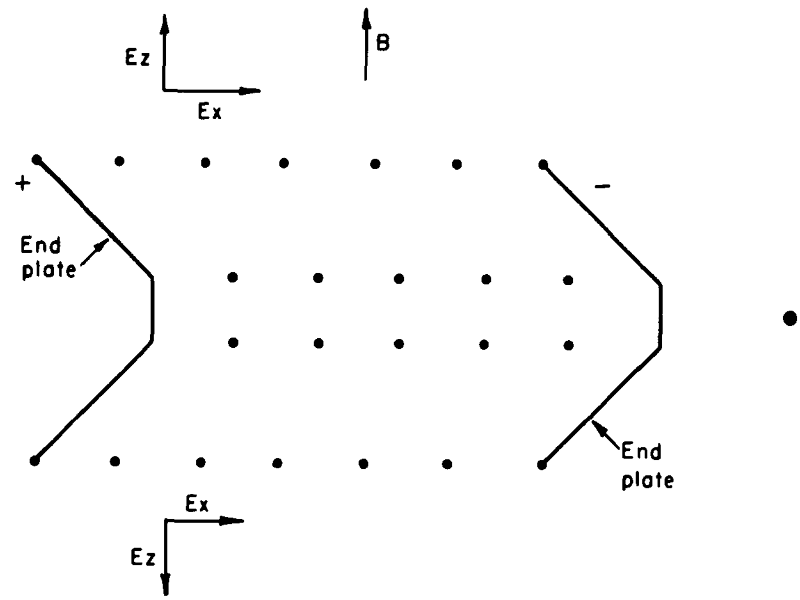

Figure 7.5. Electrode Configuration for Rectangular Delay Line.

controls the drift velocity, is substantially uniform throughout the drift space. The focussing field, E_z, on the other hand, has two discontinuities. In the central region it is zero. In the adjacent regions it has a constant magnitude, but in each case it is directed to force the electrons to the center.

An approximation to this structure has been used in the design of a new experimental model of the plasma delay line. A photograph, Fig. 7.6, shows that each end plate has been replaced by two sections which are insulated from each other. Each section is connected to the corresponding section on the other side of the device by forty-six turns of resistance wire wound on ceramic forms which are then spring loaded to prevent slackening of the wires. The wire diameter is 1×10^{-3} inches and the spacing between turns is approximately 11×10^{-3} inches. In the right half of the photograph, a coated glass rod is visible in the drift space. This resistor collects electrons, but unlike a metal conductor it does not distort the electric field. At the left is a triode launcher with a slit anode to define a sheet electron beam. Below the triode, but visible only as it emerges from the end plate, is a second coated glass rod. This resistor which serves as a source of secondary electrons is removed when the tube is operated in the plasma mode.

The model, which is free of certain field distortions present in the original tube, is assembled mostly with small nuts, bolts, and ceramic spacers. It is thus possible, by changing parts, to use different kinds of collectors, and to vary mechanical parameters such as the slit width in the triode. The tube has been mounted in the magnet, and the assembly of instrumentation for the experiments is almost complete.

H. G. Slottow

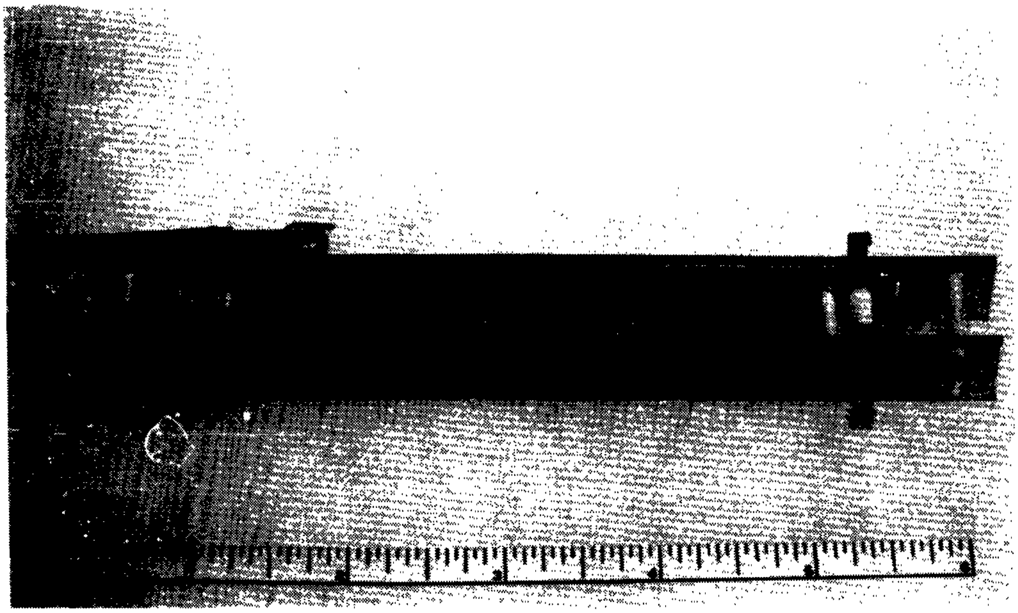

Figure 7.6. Plasma Delay Line Electrode Assembly.

8. HIGH MAGNETIC FIELD SUPERCONDUCTORS

C. B. Satterthwaite
J. O. Kopplin

'. C. Leung
R. Ries
R. Klingbiel

8.1 Introduction

This group is primarily interested in studies of superconductivity pertaining to the persistance of superconductivity in very high magnetic fields. There are three phases of this program in which work is being initiated. They are: (a) basic studies of superconducting phenomena, (b) preparation and study of materials, and (c) devices and apparatus involving superconductors.

8.2 Vanadium Study

From the single crystal of vanadium, the preparation of which was reviewed in the last progress report, two parallel sections 2.5 inches in length were cut using the spark-cutting technique. One section was cut to a 0.020 inch diameter; the other to a 0.100 inch diameter. These sections were cut by using for the opposing electrode in the spark-cutting procedure a 0.25 inch thick block into which a series of holes of decreasing diameter were machined. The single vanadium crystal was "passed" through the holes until the desired diameter was reached.

A suitable procedure for working and reducing pure vanadium to a 0.020 inch diameter wire has been developed by Fansteel Metallurgical Corporation under a joint research agreement.

Preliminary cryogenic tests of the 0.020 inch diameter single crystal indicate nearly ideal characteristics. Careful measurements of the transitions temperature, the critical field and residual resistance are planned.

Critical field measurements on highly worked 0.020 inch diameter specimens of pure vanadium indicate a highly irregular pattern.

J. O. Kopplin

8.3 Niobium-Tin Wire

In cooperation with the Fansteel Metallurgical Corporation some studies have been made of means of fabricating Nb_3Sn wire for use in superconducting solenoids and other apparatus. The metallurgical processing and fabrication have been carried out by Fansteel, and the evaluation of superconducting properties has been done by the cryogenics group.

Two batches of wire have been fabricated. A control batch, similar to the wire first developed, was made by packing a mixture of Nb and Sn powders into a Nb tube and subsequently drawing down to 0.015 inches diameter. The other batch was made by inserting into a 1/4 inch Nb tube a cable of continuous wires of Nb and Sn and drawing this composite down to 0.015 inches. It was hoped that the cable technique would lead to a large Nb-Sn interface, continuous along the wire where reaction between the two components could occur and that this structure would carry higher superconducting currents and would have more uniform and predictable superconducting properties.

Samples of both batches of wire were heat treated in vacuum at several temperatures between 700°C and 1,050°C and at times varying from 4 to 16 hours. These were evaluated by measuring the critical current as a function of magnetic field in fields varying from 0 to 22 kilogauss.

Critical currents for the wire made from the cable varied with magnetic field approximately as expected for Nb_3Sn but were lower by a factor of 2 or 3 than comparably treated control specimens. Maximum currents in the cable wire at 22 KG were about 15 amps. Of the time and temperatures selected for heat treatment 900°C for 16 hours seemed to be optimum.

Recently developed metalographic techniques applied to these wires indicate that far less intimate contact between Nb and Sn was achieved in the cable than expected. Means of increasing the Nb-Sn interface are being sought.

R. Klingbiel
R. Ries
C. B. Satterthwaite

8.4 Preparation of Crystalline Nb_3Sn

A number of experiments have been conducted using the induction furnace described earlier for the preparation of crystalline Nb_3 Sn. In a graphite crucible a melt of Sn was maintained at a temperature of 1000°C to 1250°C in intimate contacts with Nb granules for an extended period of time to obtain a saturated solution of Nb in Sn. A probe of Nb or a quartz probe carrying a seed crystal of Nb_3 Sn was lowered until it touched the surface of the melt.

With the Nb probe, because of the metallic thermal conductivity of the Nb, a cool spot was presented at the surface of the liquid to provide a point of nucleation. In all cases nucleation occurred and clusters of crystal formed with some dendritic growth along the surface indicating that radiation cooled the surface. With the seed crystal growth was still in clusters without growth of any large single crystal, however, by both methods crystal faces several tenths of a millimeter have formed.

X-ray analysis of crystals grown from melts at 1000°C to 1250°C has indicated that the polycrystalline clusters are pure Nb_3 Sn.

Work is in progress to vary conditions to encourage growth of larger and more perfect crystals.

W. C. Leung

9. VACUUM ELECTRICAL BREAKDOWN

E. M. Lyman
F. Konrad
T. Casale
H. E. Tomaschke

9.1 Refinements of Preliminary Measurements

The preliminary measurements[1] on vacuum breakdown between parallel tungsten electrodes have been repeated with great care to include the effect of the power supply ripple on peak voltages applied to the electrodes and the resulting peak field emission currents. The Fowler-Nordheim plots of log i/V^2 vs. $1/V$ are, as before, essentially straight lines over the entire range of emission current (5 to 6 orders of magnitude). Defining the breakdown voltage as the applied potential difference at which the first visible bright spark or arc occurs between the electrodes, the critical field at the cathode for each of the breakdown points was calculated from the breakdown voltage and the field enhancement factor due to surface irregularities (as calculated from the slope of the corresponding Fowler-Nordheim plot). The critical field calculated in this manner was found to be essentially independent of electrode spacing over the entire range studied; $5 \times 10^{-3} < d < 0.41$ cms., with a mean value of 6.5×10^7 volts/cm. The mean of the previously reported values was 7.6×10^7 volts/cm.

In some of the cases there is a deviation of the observed value of i/V^2 from the straight line predicted by the Fowler-Nordheim equation in the region of large currents just prior to breakdown. The deviation is toward higher currents than prediced and is in the general direction observed by Gofman[2]. The greatest deviation observed was by a factor of 2. About half of the F-N plots showed no deviation.

Sharp, faint spots of blue light are observed on the anode at voltages less than the breakdown voltages. These are thought to be due to impinging electron beams which originate at the surface irregularities on the cathode. At voltages just below breakdown there may be dozens of such spots per cm^2. Similar spots

---

[1] Coordinated Science Laboratory. Progress Report for June, July, August, 1962. p. 72

[2] I. I. Gofman, O. D. Protopopov and G. N. Shuppe, Soviet Physics Solid State Physics 2, 1203 (1960).

were observed by Little, Smith, and Arnett[3], and point sources of x-rays coming from extended anodes and cathodes have been observed by Singer and Doolittle.[4] It seems reasonable to conclude that for extended electrodes, the prebreakdown current originates from many points on the cathode, and that at breakdown arcing occurs from one or more of these points, possibly due to the mechanism postulated by Dyke[5] and extended by Alpert and Lee.[6]

E. M. Lyman
F. Konrad
T. Casale

9.2 Electron Microscope Studies

Continued studies of the cathode surface with an electron microscope have shown the following:

1) There are projections or "whiskers" on the cathode surface (see Fig. 9.1).

2) One or more of these whiskers disappear after electrical breakdown.

It should be noted that for these studies "breakdown" is defined as the point at which the field-emission current suddenly changes, either increasing or decreasing, while the voltage is constant. This change in current is usually 50 per cent or greater. Typically this is not accompanied by a visible discharge as in the usual definition of breakdown (as, for example, in Lyman's work).

When the cathode tip has been smoothed by heating to about 2000° C., the field enhancement factor as calculated from a Fowler-Nordheim plot[1] is about 20. After one or more breakdowns this factor increases to 50 or greater with some values as high as 300. The calculated emitting areas range from 10^{-9} to 10^{-14} cm^2. Enhancement factors and areas calculated from electron micrographs are in rough agreement with those calculated from the Fowler-Nordheim plots. Since an electron micrograph gives only one profile of the cathode surface it is possible that only part of a whisker may be seen. Thus, accurate calculations cannot be made by this method.

---

3 Little, Smith and Arnett, NRL Report No. 5671, Oct. 2, 1961.

4 B. Singer and H. D. Doolittle. Private communication.

5 W. Dyke. See, for example, Phys. Rev. 91, 1043 (1953).

6 D. Alpert and D. Lee. Coordinated Science Laboratory Report R-129, June 7, 1962.

There are several factors or phenomena which are not understood at present. One of these is the large variation in the current density calculated at the breakdown points. The values of current density range from 1×10^{0} to 2×10^{8} amp/cm^2. According to the mechanism proposed by Dyke[7], breakdown should occur at a critical current density of approximately 10^{8} amp/cm^2. The large variation can be partially explained by the difference in the geometry of Dyke's model and that of the observed whiskers.

Another phenomenon is a break in the Fowler-Nordheim plot such that the plot consists of two intersecting straight lines as shown in Figure 9.2. This phenomenon is found only occasionally; but when it is found, it is reproducible provided no breakdown occurs.

H. E. Tomaschke

---

[7] W. P. Dyke and J. K. Trolan, Phys. Rev. 89, 799 (1953).

Figure 9.1 (a). Electron micrograph of entire cathode tip.

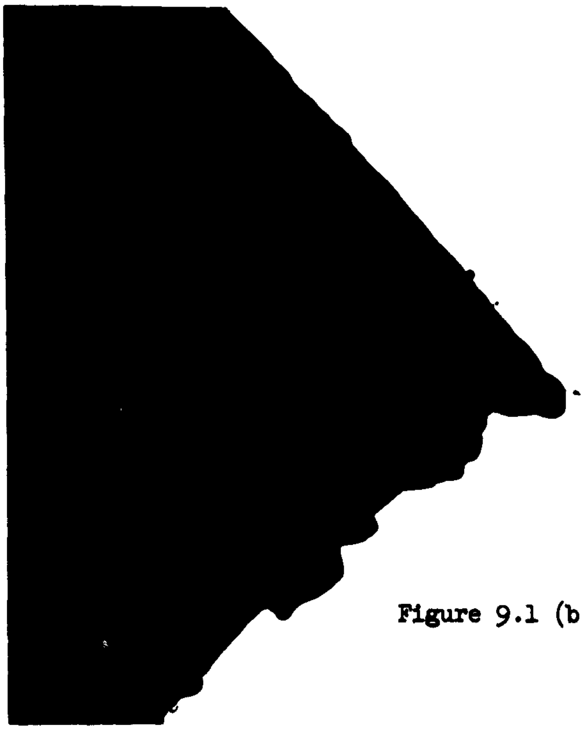

Figure 9.1 (b). Enlarged view of one section.

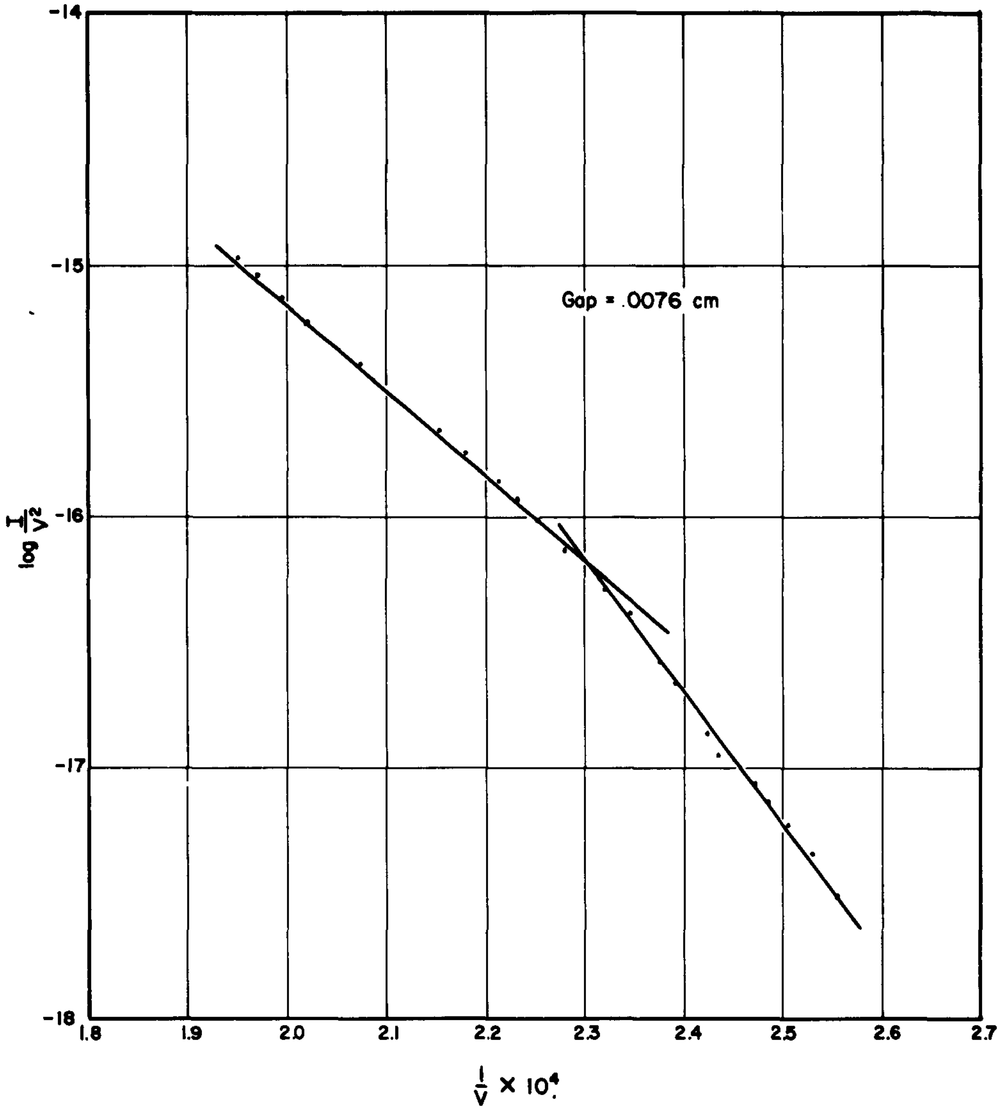

Figure 9.2. Fowler-Nordheim Plot.

10. PHYSICAL ELECTRONICS

R. N. Peacock George Riddle

10.1 Evaporated Thin Films

The principal effort during this quarter has been directed toward study of the voltage-current characteristics of metal-oxide-metal film sandwiches. In contrast to the reports of some investigators, negative resistance has been observed to frequencies of at least several hundred cycles per second, and with the samples in air as well as in vacuum. Measurements have been made with SnO_2 as well as with the Al_2O_3 used earlier. Sandwich structures made with insulating tin oxide have properties similar to those with aluminum oxide. Tin oxide films prepared by sputtering tin in tank helium or air have very good dielectric properties.

The receipt of a Varian VI-4 vacuum system in March, 1963 is expected to aid in the clean preparation and measurement of films.

R. N. Peacock
G. Riddle

11. ARMS CONTROL AND DISARMAMENT RESEARCH

B. L. Hicks C. B. Satterthwaite

The part-time activities of several members of the staff during the past quarter have reflected their interest in encouraging the growth of ACD research at the University of Illinois. Among these activities were:

a) attendance of Drs. Satterthwaite and Hicks at the International Arms Control Symposium at the University of Michigan, December 17-20, 1962;

b) formation, with the help of faculty from several other departments, of a weekly, interdepartmental Seminar on Arms Control and Disarmament Research;

c) discussion with scientists of the U.S. Arms Control and Disarmament Agency about that Agency's programs of research and of research support.

One purpose of these activities is to provide background for finding ACD research problems which conform to our professional interests and capabilities.

B. L. Hicks
C. B. Satterthwaite

DISTRIBUTION LIST AS OF NOVEMBER 7, 1962

1 Director
Air University Library
Maxwell Air Force Base, Alabama
Attn: CR-4803a

1 Redstone Scientific Information Center
U.S. Army Missile Command
Redstone Arsenal, Alabama

2 Hughes Aircraft Company
Florence and Teale
Culver City, California
Attn: N.E. Devereux
Technical Document Center

3 Autonetics
9150 East Imperial Highway
Downey, California
Attn: Tech. Library, 3041-11

1 Dr. Arnold T. Nordsieck
General Motors Corporation
Defense Research Laboratories
6767 Hollister Avenue
Goleta, California

1 Inspector of Naval Material
Los Angeles, California
Transmittal to:
Litton Systems, Inc.
5500 Canoga Avenue
Woodland Hills, California
Attn: Engineering Library

1 Sylvania Electronic Systems - West
Electronic Defense Laboratories
P. O. Box 205
Mountain View, California
Attn: Documents Center

1 Varian Associates
611 Hansen Way
Palo Alto, California
Attn: Dr. Ira Weissman

1 Huston Denslow
Library Supervisor
Jet Propulsion Laboratory
California Institute of Technology
Pasadena, California

1 Space Technology Labs, Inc.
One Space Park
Redondo Beach, California
Attn: Acquisitions Group
STL Technical Library

2 Commanding Officer and Director
U.S. Naval Electronics Laboratory
San Diego 52, California
Attn: Code 2800, C.S. Manning

1 Commanding Officer and Director
U.S. Navy Electronics Laboratory
San Diego 52, California
Attn: Library

1 Office of Naval Research Branch Office
1000 Geary Street
San Francisco, California

1 Stanford Electronics Laboratories
Stanford University
Stanford, California
Attn: SEL Documents Librarian

1 AFRST - SC
Headquarters, USAF
Washington 25, D. C.

1 Director of Science and Technology
Headquarters, USAF
Washington 25, D. C.
Attn: AFRST-EL/GU

1 Headquarters, R & T Division
Bolling Air Force Base
Washington 25, D. C.
Attn: RTHR

1 Headquarters, U.S. Army Materiel Command
Research Division, R & D Directorate
Washington 25, D. C.
Attn: Physics & Electronics Branch
Electronics Section

1 Commanding Officer
Diamond Ordnance Fuze Laboratories
Washington 25, D. C.
Attn: Librarian, Room 211, Bldg. 92

1 Operations Evaluation Group
Office of the CNO (Op03EG)
Navy Department
Washington 25, D.C.

1 Chief of Naval Operations
Tech. Analysis & Advisory Group (OP-07T)
Pentagon
Washington 25, D. C.

1 Commanding Officer & Director
David W. Taylor Model Basin
Navy Department
Washington 7, D. C.
Attn: Code 142, Library

1 Bureau of Ships
Department of the Navy
Washington 25, D. C.
Attn: Code 686

1 Bureau of Ships
Navy Department
Washington 25, D.C.
Attn: Code 732

1 Technical Library, DLI-3
Bureau of Naval Weapons
Department of the Navy
Washington 25, D. C.

1 Director
Naval Research Laboratory
Washington 25, D.C.
Attn: Code 5140

1 Department of the Navy
Office of Naval Research
Washington 25, D.C.
Attn: Code 437

1 Dr. H. Wallace Sinaiko
Institute for Defense Analyses
Research & Engineering Support Division
1666 Connecticut Ave., N.W.
Washington 9, D.C.

1 Data Processing Systems Division
National Bureau of Standards
Conn. at Van Ness
Room 239, Bldg. 10
Washington 25, D.C.
Attn: A.K. Smilow

1 Exchange and Gift Division
The Library of Congress
Washington 25, D.C.

1 NASA Headquarters
Office of Applications
400 Maryland Avenue, S.W.
Washington 25, D.C.
Attn: Mr. A. M. Greg Andrus
Code FC

1 APGC (PGAPI)
Eglin Air Force Base
Florida

1 Martin Company
P.O. Box 5837
Orlando, Florida
Attn: Engineering Library
MP-30

1 Commanding Officer
Office of Naval Research, Chicago Branch
John Crerar Library Building
10th Floor, 86 East Randolph Street
Chicago 1, Illinois

1 Librarian
School of Electrical Engineering
Purdue University
Lafayette, Indiana

2 Keats A. Pullen, Jr.
Ballistic Research Laboratories
Aberdeen Proving Ground, Maryland

1 Research Analysis Corporation
6935 Arlington Road
Bethesda 14, Maryland
Attn: Library

5 Scientific & Technical Information Facility
P. O. Box 5700
Bethesda, Maryland
Attn: NASA Representative (S-AK/DL)

1 Commander
Air Force Cambridge Research Laboratories
Laurence G. Hanscom Field
Bedford, Massachusetts
Attn: CRXL

1 Research Laboratory of Electronics
Massachusetts Institute of Technology
Cambridge 39, Massachusetts
Attn: Document Room, 26-327

1 Lincoln Laboratory
Massachusetts Institute of Technology
P.O. Box 73
Lexington 73, Massachusetts
Attn: Library, A-082

1 Sylvania Electric Products Inc.
Electronic Systems
Waltham Labs. Library
100 First Avenue
Waltham 54, Massachusetts

1 Minneapolis-Honeywell Regulator Co.
Aeronautical Division
2600 Ridgeway Road
Minneapolis 13, Minnesota
Attn: Mr. D. F. Elwell
Main Station: 625

1 Inspector of Naval Material
Bureau of Ships Technical Representative
1902 West Minnehaha Avenue
St. Paul 4, Minnesota

20 Activity Supply Officer
Building 2504
Charles Wood Area
Fort Monmouth, New Jersey
Marked: For Office of Engineering Operations
Order No. 39578-PM-60-91-91

1 Radio Corporation of America
RCA Laboratories
David Sarnoff Research Center
Princeton, New Jersey
Attn: Library

1 Dr. J. H. Frank
861 Washington Avenue
Westwood, New Jersey

1 Mr. A. A. Lundstrom
Bell Telephone Laboratories
Room 2E-127
Whippany Road
Whippany, New Jersey

1 AFMDC (MDSGP/Capt. Wright)
Holloman Air Force Base
New Mexico

1 Mailing Zone C-67
Bell Aerosystems Company
P. O. Box 1
Buffalo 5, New York
Attn: Technical Library

1 Cornell Aeronautical Laboratory, Inc.
4455 Genesee Street
Buffalo 21, New York
Attn: J. P. Desmond, Librarian

1 Sperry Gyroscope Company
Marine Division Library
155 Glen Cove Road
Carle Place, L.I., New York
Attn: Mrs. Barbara Judd

1 Rome Air Development Center
Griffiss Air Force Base, New York
Attn: Documents Library
RAALD

1 General Electric Company
Advanced Electronics Center
Cornell University
Ithaca, New York
Attn: F. Kuehn, Librarian

1 Library
Light Military Electronics Department
General Electric Company
Building No. 28-501
Schenectady 5, New York

3 Commanding Officer
U.S. Army Research Office (Durham)
Attn: CRD-AA-IP, Mr. Ulsh
Box CM, Duke Station
Durham, North Carolina

1 Goodyear Aircraft Corporation
For: Project MX 778
Akron 15, Ohio

1 Battelle-DEFENDER
Battelle Memorial Institute
505 King Avenue
Columbus 1, Ohio

1 ASD (ASNC)
Wright-Patterson Air Force Base
Ohio

1 ASD (ASRNG)
Wright-Patterson Air Force Base
Ohio

1 Commanding Officer (AD-5)
U.S. Naval Air Development Center
Johnsville, Pennsylvania
Attn: NADC Library

2 Commanding Officer
Frankford Arsenal
Philadelphia 37, Pennsylvania
Attn: SMUFA-1300

1 General Atronics Corporation
1075 DeHaven Street
West Conshohocken, Pennsylvania
Attn: Miss D. M. Keener
Librarian

1 H. E. Cochran
Oak Ridge National Laboratory
P. O. Box X
Oak Ridge, Tennessee

1 President
U.S. Army Air Defense Board
Fort Bliss, Texas

1 U.S. Air Force Security Service
San Antonio, Texas
Attn: ODC-R

1 ASTIA Technical Library AFL 2824
Arlington Hall Station
Arlington 12, Virginia
Attn: TISLL

1 U.S. Naval Weapons Laboratory
Computation and Analysis Laboratory
Dahlgren, Virginia
Attn: Mr. Ralph A. Niemann

2 Army Materiel Command
Research Division
R & D Directorate
Bldg. T-7
Gravelley Point, Virginia